Influence of temperature and upwelling intensity on oil sardine (*Sardinella longiceps*) landings along the southwest coast of India

30 April, 2018

Introduction

The Indian oil sardine (*Sardinella longiceps* Valenciennes, 1847) is one of the most commercially important fish resources along the southwest coast of India (Figure 1) and comprises ca 25% of the catch biomass (Vivekanandan et al. 2003). Landings of the Indian oilsardine are highly seasonal and peak during and after the summer monsoon period (June through September), in conjunction with the onset and early relaxation of coastal upwelling. However, the landings of this small pelagic finfish are also highly variable from year to year. Small pelagics often exhibit high variability due to the effects of environmental conditions on survival and recruitment (Checkley Jr. et al. 2009). In addition, the Indian oil sardine fishery is largely coastal and artisanal thus migration of fish schools in and out of the coastal zone greatly affects exposure to the fishery.

Researchers have examined a variety of environmental variables for their correlation with landings of the Indian oil sardine. Precipitation during the southwest monsoon (Murty and Edelman 1966, Antony Raja 1969, 1972, Jayaprakash 2002) and the day of the monsoon arrival (Jayaprakash 2002) have been widely examined and correlations found, but the reported effects are positive in some studies and negative in others. Precipitation is correlated with monsoon winds which trigger upwelling but may also affect salinity and act as a direct or indirect cue for spawning. Researchers have also found correlations with various metrics of upwelling intensity during the post-monsoon period (Longhurst and Wooster 1990, Madhupratap et al. 1994, Jayaprakash 2002, Krishnakumar et al. 2008, Thara 2011) and with direct measures of productivity, such as nearshore zooplankton and phytoplankton abundance (Hornell 1910, Nair 1952, Nair and Subrahmanyan 1955, Madhupratap et al. 1994, George et al. 2012). Researchers have also found correlations with sea surface temperature (SST); SST can affect both somatic growth rates and juvenile survival but also can cause fish to move off-shore and away from the shore-based fishery (Annigeri 1969, Prabhu and Dhulkhed 1970, Pillai 1991).

In this paper, we revisit the analysis of environmental covariates that correlate with oil sardine catch using data from 1983 to 2015 on seasonal landings and environmental conditions from remote-sensing. Based on biological information concerning how environmental conditions in the coastal waters affect spawning density, exposure of sardines to the coastal fishery, and larval and juvenile sardine survival, we develop a set of hypotheses about which remote-sensing covariates should correlate with current or future landings. We use generalized additive modelling of the landing data with remote-sensing covariates to test for these correlations.

Study area and oil sardine life history

Our analysis focuses on the Kerala coast (Figure 1) region of India, where the majority of the Indian oil sardines are landed and where oil sardines comprise ca. 40% of the marine fish catch (Srinath 1998, Vivekanandan et al. 2003). This area is in the Southeast Arabian Sea (SEAS), one of world's major upwelling zones, with seasonal peaks in primary productivity driven by upwelling caused by winds during the Indian summer monsoon (Madhupratap et al. 2001, Habeebrehman et al. 2008) between June and September. Within the SEAS, the coastal zone off Kerala between 9°N to 13°N has especially intense upwelling due to the combined effects of wind stress and remote forcing (Smitha et al. 2008, Smitha 2010). The result is a strong temperature differential between the near-shore and off-shore and high primary productivty and chlorophyll in this region (Madhupratap et al. 2001, Habeebrehman et al. 2008, Jayaram et al. 2010, Raghavan et al. 2010, Smitha 2010, Chauhan et al. 2011). The primary productivity peaks subside after September while mesozooplankton abundances increase and remain high in the inter-monsoon period (Madhupratap et al. 2001).

The life cycle of the oil sardine fishery begins with the entry of adult fish into the inshore areas during June – July, corresponding with the onset of the southwest monsoon (Chidambaram 1950, Antony Raja 1969) and restricted along the narrow strip of the western India continental shelf, within 20 km from the shore. The fish migrate from offshore to coastal waters and vice versa coinciding with the prevailing wind conditions (Hornell 1910). A gradual increase in temperature ranging from 26 to 28°C is favorable for their inshore migration (Chidambaram 1950). According to Nair et al. (2016), the exact location of oil sardine spawning grounds along the Indian coastline is still unclear; however, it is generally believed that the spawning of oil sardine occurs during the southwest monsoon period (Jun-Jul) when temperature, salinity and suitable food availability are conducive for larval survival (Murty and Edelman 1966, Jayaprakash and Pillai 2000, Krishnakumar et al. 2008), although some studies suggest that spawning can occur as late as September (Hornell 1910, Hornell and Nayudu 1923, Antony Raja 1969, Prabhu and Dhulkhed 1970).

After eggs are spawned, they develop rapidly into larvae within 24 hrs (Nair 1959). The phytoplankton bloom that provides for sardine larvae food is dependent upon nutrient influx from coastal upwelling and runoff from rivers. The blooms start in the south in June, increase in intensity and spread northward up the coast (Smitha 2010). Oil sardines grow rapidly during their first few months and can reach 40mm with 2 months (reference). Variation in the bloom initiation time and intensity lead to changes in the food supply to sardine larvae and corresponding changes in their growth rate and survival and the later recruitment of 0-year sardines into the fishery (George et al. 2012). During March to May, the inshore waters warm considerably and sardines move off-shore to deeper waters (Chidambaram 1950). Catches of sardines are correspondingly low during this time for all size classes.

The age at first maturity occurs at less than one year, at about 150 mm size. Spawning begins during the southwest monsoon period (June-July) when temperature, salinity and suitable food availability are conducive for larval survival and continues into September (Murty and Edelman 1966, Jayaprakash and Pillai 2000, Krishnakumar et al. 2008). The fishery is closed during June to mid-July during the monsoon and peak spawning, and when it resumes in mid-July, it is dominated by 1-2.5 year old fish that have recently spawned (spent). In August a spike of 0-year (40mm) juveniles from the June spawning ofter appears in the catch and another spike of 0-year fish is sometimes seen in February from the last fall spawning. Overall, catches along the Kerala coast are fairly high throughout the year except during March-May (Figure 2).

Hypotheses

Based on biological information concerning how environmental conditions affect sardine survival and recruitment and affect exposure of sardines to the coastal fishery, we developed a set of hypotheses about which remote-sensing covariates in which months should correlate with landings in specific quarters.

Quarter 3 July-Sept catch correlates

Quarter 3 is during the summer monsoon, with the peak in June and continuing at a lower level into October. During this time, sardines move inshore from offshore and become exposed to the primarily coastal fishery. Factors that affect inshore migration or spawning should affect the catch in quarter 3, which is primarily of mature fish although small (40mm) juveniles from the June spawning often appear befiefly in the catch during August. The following are the major factors that are hypothesized to affect the catch in quarter 3 due to either a stronger spawning class or higher (or lower) exposure of the spawning age fish to the fishery due to higher (or lower) inshore migration.

1. Precipitation low or high during either the summer monsoon (June-July) or pre-monsoon (Apr-May) is associated with low spawning.

2. Low sea surface temperature is associated with delayed and limited spawning in Pacific sardines (Jacobson and MacCall 1995). The reasons for this may be behavioral as low temperature as associated with poor survival of larvae. Larval mortality rates may be higher in colder water due to increased zooplankton predation and upwelling (associated with cold surface temperatures) advects larvae into offshore waters.

3. In addition to advection of larvae offshore, upwelling brings low oxygen water to the surface which discourages inshore migration to coastal spawning areas. Thus due to both lower SST and lower dissolved oxygen, strong upwelling during the spawning season is expected to be negatively associated with the spawning biomass in the near-shore region.

4. Salinity is also associated with spawning initiation; however we do not have long-term salinity data.

5. Spawners are age 2+ fish, thus the biomass in the previous two seasons should be correlated with the biomass of spawners this year. This should especially be the case for the biomass in quarters 4, 1 and 2 of the previous season as these were age 1-2 fish. A stronger cohort of age 1-2 fish in the previous year should be associated with a stronger spawner class in the current year. Note that it could also be the case that higher catch of age 1-2 fish in the previous season would be associated with lower spawners in the current year due to depletion. However during the majority of our study period, the fishery was largely artisanal and is not thought to be sufficient to deplete the population.

Post-summer monsoon catch correlates

After spawning, during the 4th quarter of the current calendar year and the 1st and 2nd quarters of the next calendar year, the length distribution of the catch first shifts to smaller fish as 0-year juveniles begin shoaling inshore. The catch during the post-monsoon part of the season should be correlated with factors associated with increased survival of eggs and larvae the current and previous years.

1. Sea surface temperature is associated with egg and larval survival (Jacobson and MacCall 1995).
2. Upwelling is associated with higher productivity and higher density of zooplankton, which leads to better larval and juvenile growth and survival. Thus the strength of upwelling during the post-spawning quarters should be associated with higher non-spawning biomass in subsequent years.
3. Chlorophyll blooms are signatures of high productivity from nutrient influx either due to upwelling or coastal inputs. Thus the bloom intensity in prior years should be associated with future non-spawning biomass. In addition, juveniles shoal in response to chlorophyll blooms (citation) and thus the near shore chlorophyll bloom intensity in the current season should be associated with higher post-spawning catches due to higher exposure of the non-spawning biomass to the coastal fishery.

1 Abundance of 1-year and 2-year fish should be correlated with strength of the cohorts from the previous two seasons. We do not have have direct measures of recruitment or spawners. However the catch in quarter 3 is dominated by mature fish, thus catch in quarter 3 in the previous two calendar years is expected to be correlated with the post-monsoon catch after the summer monsoon (quarter 4 of the current calendar year with quarter 1 and 2 of the next calendar year).

1. Because age 2 fish also appear in the catch after quarter 3, we also expect the post-monsoon catch in the previous season to be correlated with the post-spawning catch in the current season.

Methods and data

Sardine landing data

Quarterly fish landing data have been collected by the Central Marine Fisheries Research Institute (CMFRI) in Kochi, India, since the early 1950s using a stratified multi-stage sample design that takes into account landing centers, number of fishing days, and boat net combinations in fishing operations (Srinath et al. 2005). The quarterly landings for oil sardine landed from all gears in Kerala were obtained from CMFRI reports (1956-1984) and online database (1985-2015). (CMFRI 1969, 1995, Pillai 1982, Jacob et al. 1987, 2016). The quarterly landing data were log-transformed to stabilize the seasonal variance.

Remote-sensing data

We analysed monthly composites of the following environmental data derived from satellites: Sea Surface Temperature (SST), chlorophyll-a (CHL), upwelling (UPW) and precipitation. Sea surface temperature: For 1981 to 2002, we used Pathfinder Version 5.2 product on a 4km grid, and for 2003 to 2016, we used Advanced Very-High Resolution Radiometer (AVHRR) data at a 0.1 degree spatial scale. Chlorophyll-a, we used SeaWiFS data on a 0.1 degree spatial scale for 1981 to 2002 and MODIS data from 2003 to 2017 at 0.05° spatial scale. The SST and CHL data were averaged across thirteen 1 degree by 1 degree boxes which roughly parallel the bathymetry (Figure 1). The SST and CHL satellite data were retrieved from the NOAA ERDDAP server.

For an index of coastal upwelling, we used the sea-surface temperature differential between near shore and 3 degrees offshore as described by Naidu et al. (1999) and Smitha et al. (2008). The index is computed as the average SST in boxes 3 degrees offshore of boxes 1-5 in Figure 1 minus the average SST in boxes 1-5. For SST, we used the remote-sensing sea-surface temperature data sets described above. This SST-based upwelling index has been validated as a more reliable metric of upwelling off the coast of Kerala compared to wind-based upwelling indices (Smitha et al. 2008).

Precipitation data were obtained from two different sources. The first was an estimate of the monthly precipitation (mm) over Kerala from land-based rain gauges (Kothawale and Rajeevan 2017). This time series is available from the start of our landing data (1956). The second was a remote-sensing precipitation product from the NOAA Global Precipitation Climatology Project (Adler et al. 2016). This provides estimate of precipitation over the ocean using a global 2.5 degree grid. We used the 2.5 by 2.5 degree box defined by latitude 8.75 to 11.25 and longitude 73.25 to 75.75 for the precipitation off the coast of Kerala. These data are available from 1979 forward (2017).

Explanatory models

We investigated correlations between environmental variables and sardine catch during spawning and post-spawning periods using generalized additive models (GAMs, Wood 2017). GAMs allow one to model the effect of a covariate as a flexible non-linear function and it was known that the effects of the environmental covariates were likely to be non-linear, albeit in an unknown way. Our approach is similar to that taken by Jacobson and MacCall (1995) in a study of the effects of SST on Pacific sardine recruitment.

The model for catch in quarter 3 was of the form

$$ln(S_t) = \alpha + f_1(c_1) + f_2(c_2) + s_1(ln(C_{t-1})) + s_2(ln(C_{t-2})) + \varepsilon$$

where $ln(S_t)$ is the log catch in the 3rd quarter of year t. Catch in the 3rd quarter (July-Aug) captures mainly spawning age fish as it overlaps with the tail end of the spawning season—the fishery is closed July to mid-August during the height of the summer monsoon and spawning season. The model seeks to explain the variability in catch in the 3rd quarter via a non-linear function of the covariates, c_1 and c_2, plus a non-linear function of total catch in prior years. The catches were logged to stabilize and normalize the variance. The model is primarily statistical, meaning it should not be thought of as being a population growth model. It is a form of model that is often used for modelling the effects of covariates on the number of fish that recruit into the fishery (e.g. Jacobson and MacCall 1995, add others or a textbook). The covariates tested are those discussed in the section on covariates that have been hypothesized to drive the size of the spawning biomass exposed to the fishery. The relevant covariate may be in the concurrent with the catch or in a prior year.

The model for catch in the non-spawning quarters (October to June) took a similar form

$$ln(N_t) = \alpha + f_1(c_1) + f_2(c_2) + s_1(ln(S_{t-1})) + s_2(ln(N_{t-1})) + \varepsilon$$

where $ln(N_t)$ is the log of the total catch in the post-spawning season October to June (a ninemonth period that spans two calendar years). We included the catches during the spawning season (S_t) separately from the non-spawning season (N_t). The covariates that affect the egg and larval survival may be quite different from those affecting the age-1 to age-2 or age-2 to age-3 survival. We wanted to be able to model these separately. The covariates tested are those discussed in the section on covariates that have been hypothesized to drive both survival and growth of juvenile fish and the factors that lead migration of fish inshore and thus exposed to the coastal fishery.

Model selection was conducted in a step-wise fashion. The length of the covariate data was 33-35 years (1982 to 2015 or 2017) for most covariates and this was not sufficient for fitting all covariates simultaneously. The model for the effect of the past of biomass on current biomass (density-dependence) was first determined. Once a sufficient model for the density-dependence was determined, the covariates were studied individually and then jointly. F-tests and AIC on nested sets of GAM models (Wood et al. 2016) were used to evaluate the support for models. One feature of GAMs is that they allow the ‘flexibility’ or smoothing parameter of the response curve to be estimated. However we fixed the degree of flexibility so that reasonably smooth responses were achieved. Multi-modal or overly wiggly response curves would not make sense for our covariates. We used GAMs with smooth terms represented by penalized regression splines (Wood 2011, using the mgcv package in R) and fixed the smoothing term at an intermediate value.

Results

Catches in prior seasons as explanatory variables

There was support for including the post-spawning catch in the previous year as an explanatory variable for the catch during the spawning season (3rd quarter). Models with $ln(N_{t-1})$ were strongly supported over an intercept only model (Table 1, time-dependency test). However the addition of the catch two years prior, $ln(N_{t-2})$, lead to either no decrease in the residual deviance (i.e. increase in the explained variance) and in fact, increased the residual deviance for the model with non-linearity (Table 1, Linearity test). We also tested the support for non-linearity in the effect of the prior year catch on the catch in the spawning season. This was done by comparing models with $ln(N_{t-1})$ included as a linear term or as a non-linear function $s(ln(N_{t-1}))$ (Table 1, Linearity test). The residual deviance decreased using a non-linear response however the cost was 1.4 degrees of freedom. The result was only weak (non-significant) support for allowing a non-linear response. The full set of models tested, including tests using catch during the spawning months in previous seasons as a covariate are shown in Tables A1 and A2. The results were the same if we used the full landings data set from 1956 to 2015 (Table A3). Overall, the landings in prior seasons was only weakly explanatory for the catch in the spawning months, and the maximum R^2 was less than 30% (Table 1).

The results were similar for models of the landings during the non-spawning months (N_t) of the sardine season (Table 2). The most supported model for N_t used a non-linear response to landings during the non-spawning months of the previous season: $ln(N_t) \sim ln(N_{t-1})$ with a non-linear response to landings during the spawning months two seasons prior (Table 2). There was low support for including landings from the non-spawner months two seasons prior or for using the landings during the spawning months in the prior season (Tables A4, A5, and A6).

Environmental covariates as explanatory variables

There was no support for using precipitation during the summer monsoon (Jun-Jul) or pre-monsoon period (Apr-May) as an explanatory variable for the catch during the spawning months (Table B1) nor the non-spawning months (Table B2). This was the case whether precipitation in the current or previous season was used, if precipitation was included as non-linear or non-linear effect, or if the smoothing term (degree of non-linearity allowed) was estimated and thus not constrained, and if either precipitation during monsoon (Jun-Jul) or pre-monsoon (Apr-May) were used as the covariate.

However, we found significant correlation between average sea surface temperature during the early post-spawning period (Jul-Dec) and catch during the spawning season (Table 3, Table B3). Sea surface temperature has been found to be correlated with sardine biomass in a number of other studies [Jacobson and MacCall (1995); add the others]. The residual deviance was lowest in a model with SST in both the prior year and two years prior included and with a non-linear response for both. This a similar result to Jacobson and MacCall (1995) who found that SST in multiple prior years was supported as explanatory variables for sardine recruitment and productivity. However the reduction in degrees of freedom was high for this model and it was not supported, despite having the lowest residual degrees of freedom, given the cost (loss of degrees of freedom). The model with the lowest AIC was a model with only the current year and a non-linear response. The response shows a step-response with a negative effect at low temperatures and then an increased effect a higher temperatures (Figure 3). This type of step-response has been found in studies of the effect of SST on recruitment in Pacific sardines

(Jacobson and MacCall 1995). The R^2 for this model was 0.40 (Table 3).

The strongest predictor of the catch during the spawning season however was the upwelling strength during Jan-Mar (4-6 months prior) in the previous season (Tables 3 and B4). Jan-Mar is a period when the young of the year and age-1 fish would be found feeding in large shoals in the coastal region. This is also the time of year with the second highest catches and catches that are dominated by small-sized fish (*citation*). The best supported model included only the upwelling strength in the prior year, without SST included as a covariate (Table 3). The R^2 for this model was 0.60 and the fitted versus observed catches for this model are shown in Figure 4.

For catch in the non-spawning months (Oct-Jun), sea surface temperature during the spawning months in the current season was a significant predictor similar to what was found for catches in the spawning months. Upwelling in the prior season was also a significant predictor, but the important months were Oct-Dec. This is period is important for larval and early juvenile survival and growth, and other studies have also found this to be a critical period for future stock size in sardines (*citation*). The model with the lowest residual variance and lowest AIC was the model which included both the SST and upwelling covariates (Table 3). The R^2 for this model was 0.73 and the fitted versus observed catches for this model are shown in Figure 4.

Chlorophyll-a density is speculated to be an important predictor of larval sardine survival and growth. In addition, sardines shoal in response to coastal chlorophyll blooms, which brings them in contact with the coastal fisheries. Thus Cholorophyll-a density is assumed to be an important either covariate or driver of future or current sardine catches. However, we had chlorophyll-a remote-sensing data only from 1998 onward. Our simplest covariate model required 5 degrees of freedom, thus we were limited in the analyses we could conduct. In addition, the years, 1998-2014, have relatively low variability in catch sizes; the logged catch sizes during this period range from 10-11 during the spawning months and 11-12 during the non-spawning months. Second degree polynomial models were fit (Appendix C) to the average log chlorophyll-a density in the current and prior season from quarters 3 (Jul-Sep), 4 (Oct-Dec), and 1 (Jan-Mar). Chlorophyll-a density was not a significant predictor for the spawning catch for any of the tested combinations of current or prior season and quarter. The only significant effect was seen for non-spawner catches using chlorophyll-a density in Oct-Dec of the current and prior season (Table C1). This matches results which found that the upwelling index in Oct-Dec of the prior season was a predictor for the non-spawning months' catch. The upwelling index and chlorophyll-a density are both indices of low-trophic level productivity.

Discussion

Sardines in all the world's ecosystems exhibit large fluctuations in abundance (**???**, Schwartzlose et al. 2010). These small forage fish are strongly influenced by natural variability in upwelling driven by both large-scale forces, i.e. El Nino patterns, and by changes in winds and currents and in addition local conditions of temperature, salinity, and oxygen levels have both direct and indirect on sardine recruitment and survivial.

Many studies on Pacific sardines have looked at the correlation between sea surface temperture (SST) and recruitment. Temperature can have direct effect, an indirect effect on food availability or affect survival (Houde 1987). Studies in the California Current System, have found that SST explains year-to-year variability in Pacific sardine recruitment (Jacobson and MacCall 1995, Checkley Jr. et al. 2009, 2017, Lindegren and Checkley Jr. 2012). Consistent with these studies, we also found that SST was the covariate that explained variability in catch anomalies (difference between the landing prediction from prior years' catches).

McClatchie et al. (2010) found no SST relationship with SST and Pacific sardine recruitment, however their analysis used a linear relationship while both other studies that found a relationship (Jacobson and MacCall 1995, Checkley Jr. et al. 2017) allowed a non-linear relationship. Both Jacobson and MacCall (1995) and Checkley et al (2017) found a step-like response function for temperature, where lower temperatures were poor and had negative effects and then at a threshold value the effect became positive. Our analysis found a similar step-like effect function (Figure).

There were three outlier years when catch were much lower than expected based on prior catches. For these years, sea surface temperature improved the model fit greatly (Figure). Need to flesh out.

Discuss density-dependence. The fact that the prior year catch had a strong explainatory value.

Finish off with implications. In California Current system, SST is used as an indicator for recruitment and is used in management of harvest.

References

Adler, R., J.-J. Wang, M. Sapiano, G. Huffman, L. Chiu, P. P. Xie, R. Ferraro, U. Schneider, A. Becker, D. Bolvin, E. Nelkin, G. Gu, and N. C. Program. 2016. Global precipitation climatology project (gpcp) climate data record (cdr), version 2.3 (monthly). Report, National Centers for Environmental Information.

Annigeri, G. G. 1969. Fishery and biology of the oil sardine at karwar. Indian Journal of Fisheries 16:35–50.

Antony Raja, B. T. 1969. Indian oil sardine. CMFRI Bulletin 16:1–142.

Chauhan, O. S., B. R. Raghavan, K. Singh, A. S. Rajawat, U. Kader, and S. Nayak. 2011. Influence of orographically enhanced sw monsoon flux on coastal processes along the se arabian sea. Journal of Geophysical Research. Oceans 116:C12037.

Checkley Jr., D. M., J. Alheit, Y. Oozeki, and C. Roy. 2009. Climate change and small pelagic fish. Edited Book, Cambridge University Press, Cambridge.

Checkley Jr., D. M., R. G. Asch, and R. R. Rykaczewski. 2017. Climate, anchovy, and sardine. Annual Review of Marine Science 9:469–493.

Chidambaram, K. 1950. Studies on the length frequency of oil sardine, sardinella longiceps cuv. & val. and on certain factors influencing their appearance on the calicut coast of the madras presidency. Proceedings of Indian Academy of Sciences 31:352–286.

CMFRI. 1969. Marine fish production in india 1950-1968. Report, Central Marine Fisheries Research Institute.

CMFRI. 1995. Marine fish landings in india during 1985-93. Report.

George, G., B. Meenakumari, M. Raman, S. Kumar, P. Vethamony, M. T. Babu, and X. Verlecar. 2012. Remotely sensed chlorophyll: A putative trophic link for explaining variability in indian oil sardine stocks. Journal of Coastal Research 28:105–113.

Habeebrehman, H., M. P. Prabhakaran, J. Jacob, P. Sabu, K. J. Jayalakshmi, C. T. Achuthankutty, and C. Revichandran. 2008. Variability in biological responses influenced by upwelling events in the eastern arabian sea. Journal of Marine Systems 74:545–560.

Hornell, J. 1910. Report on the results of a fishery cruise along the malabar coast and to the laccadive islands in 1908. Madras Fishery Bulletin 4:76–126.

Hornell, J., and M. R. Nayudu. 1923. A contribution to the life history of the indian sardine with note, on the plankton of the malabar coast. Madras Fishery Bulletin 17:129.

Houde, E. D. 1987. Fish early life dynamics and recruitment variability. American Fisheries Society Symposium 2:17–29.

Jacob, T., V. Rajendran, P. K. M. Pillai, J. Andrews, and U. K. Satyavan. 1987. An appraisal of the marine fisheries in kerala. Report, Central Marine Fisheries Research Institute.

Jacobson, L. D., and A. D. MacCall. 1995. Stock-recruitment models for pacific sardine (sardinops sagax). Canadian Journal of Fisheries and Aquatic Sciences 52:566–577.

Jayaprakash, A. A. 2002. Long term trends in rainfall, sea level and solar periodicity: A case study for forecast of malabar sole and oil sardine fishery. Journal of the Marine Biological Association of India 44:163–175.

Jayaprakash, A. A., and N. G. K. Pillai. 2000. The indian oil sardine. Pages 259–281 *in* V. N. Pillai and N. G. Menon, editors. Marine fisheries research and management. Book Section, Central Marine Fisheries Research Institute, Kerala, India.

Jayaram, C., N. Chacko, K. A. Joseph, and A. N. Balchand. 2010. Interannual variability of upwelling indices in the southeastern arabian sea: A satellite based study. Ocean Science Journal 45:27–40.

Kothawale, D. R., and M. Rajeevan. 2017. Monthly, seasonal and annual rainfall time series for all-india, homogeneous regions and meteorological subdivisions: 1871-2016. Report, Indian Institute of Tropical Meteorology.

Krishnakumar, P. K., K. S. Mohamed, P. K. Asokan, T. V. Sathianandan, P. U. Zacharia, K. P. Abdurahiman, V. Shettigar, and N. R. Durgekar. 2008. How environmental parameters influenced fluctuations in oil sardine and mackerel fishery during 1926-2005 along the southwest coast of india? Marine Fisheries Information Service T&E Series 198:1–5.

Lindegren, M., and D. M. Checkley Jr. 2012. Temperature dependence of pacific sardine (sardinops sagax) recruitment in the california current ecosystem revisited and revised. Canadian Journal of Fisheries and Aquatic Sciences 70:245–252.

Longhurst, A. R., and W. S. Wooster. 1990. Abundance of oil sardine (sardinella longiceps) and upwelling on the southwest coast of india. Canadian Journal of Fisheries and Aquatic Sciences 47:2407–2419.

Madhupratap, M., T. C. Gopalakrishnan, P. Haridas, and K. K. C. Nair. 2001. Mesozooplankton biomass, composition and distribution in the arabian sea during the fall intermonsoon:

Implications of oxygen gradients. Deep Sea Research Part II: Topical Studies in Oceanography 48:1345–1368.

Madhupratap, M., S. R. Shetye, K. N. V. Nair, and S. R. S. Nair. 1994. Oil sardine and indian mackerel: Their fishery, problems and coastal oceanography. Current Science 66:340–348.

McClatchie, S., R. Goericke, G. Auad, and K. Hill. 2010. Re-assessment of the stock–recruit and temperature–recruit relationships for pacific sardine (sardinops sagax). Canadian Journal of Fisheries and Aquatic Sciences 67:1782–1790.

Murty, A. V. S., and M. S. Edelman. 1966. On the relation between the intensity of the south-west monsoon and the oil-sardine fishery of india. Indian Journal of Fisheries 13:142–149.

Naidu, P. D., M. R. R. Kumar, and V. R. Babu. 1999. Time and space variations of monsoonal upwelling along the west and east coasts of india. Continental Shelf Research 19:559–572.

Nair, P. G., S. Joseph, V. Kripa, R. Remya, and V. N. Pillai. 2016. Growth and maturity of indian oil sardine sardinella longiceps (valenciennes, 1847) along southwest coast of india. Journal of Marine Biological Association of India 58:64–68.

Nair, R. V. 1952. Studies on the revival of the indian oil sardine fishery. Proceedings of Indo-Pacific Fisheries Council 2:1–15.

Nair, R. V. 1959. Notes on the spawning habits and early life-history of the oil sardine, sardinella longiceps cuv. & val. Indian Journal of Fisheries 6:342–359.

Nair, R. V., and R. Subrahmanyan. 1955. The diatom, fragilaria oceanica cleve, an indicator of abundance of the indian oil sardine, sardinella longiceps cuv. and val. Current Science 24:41–42.

Pillai, V. N. 1982. Physical characteristics of the coastal waters off the south-west coast of india with an attempt to study the possible relationship with sardine, mackerel and anchovy fisheries. Thesis.

Pillai, V. N. 1991. Salinity and thermal characteristics of the coastal waters off southwest coast of india and their relation to major pelagic fisheries of the region. Journal of the Marine Biological Association of India 33:115–133.

Prabhu, M. S., and M. H. Dhulkhed. 1970. The oil sardine fishery in the mangalore zone during the seasons 1963-64 and 1967-68. Indian Journal of Fisheries 17:57–75.

Raghavan, B. R., T. Deepthi, S. Ashwini, S. K. Shylini, M. Kumarswami, S. Kumar, and A. A. Lotliker. 2010. Spring inter monsoon algal blooms in the eastern arabian sea: Shallow marine encounter off karwar and kumbla coast using a hyperspectral radiometer. International Journal of Earth Sciences and Engineering 3:827–832.

Schwartzlose, R. A., J. Alheit, A. Bakun, T. R. Baumgartner, R. Cloete, R. J. M. Crawford, W. J. Fletcher, Y. Green-Ruiz, E. Hagen, T. Kawasaki, D. Lluch-Belda, S. E. Lluch-Cota, A. D. MacCall, Y. Matsuura, M. O. Nevárez-Martínez, R. H. Parrish, C. Roy, R. Serra, K. V. Shust, M. N. Ward, and J. Z. Zuzunaga. 2010. Worldwide large-scale fluctuations of sardine and anchovy populations. South African Journal of Marine Science 21:289–347.

Smitha, B. R. 2010. Coastal upwelling of the south eastern arabian sea — an integrated approach. Thesis.

Smitha, B. R., V. N. Sanjeevan, K. G. Vimalkumar, and C. Revichandran. 2008. On the upwelling of the southern tip and along the west coast of india. Journal of Coastal Research 24:95–102.

Srinath, M. 1998. Exploratory analysis on the predictability of oil sardine landings in kerala. Indian Journal of Fisheries 45:363–374.

Srinath, M., S. Kuriakose, and K. G. Mini. 2005. Methodology for estimation of marine fish landings in india. Report, Central Marine Fisheries Research Institute.

Thara, K. J. 2011. Response of eastern arabian sea to extreme climatic events with special reference to selected pelagic fishes. Thesis.

Vivekanandan, E., M. Srinath, V. N. Pillai, S. Immanuel, and K. N. Kurup. 2003. Marine fisheries along the southwest coast of india. Pages 759–792 *in* G. Silvestre, L. Garces, I. Stobutzki, C. Luna, M. Ahmad, R. A. Valmonte-Santos, L. Lachia-Alino, P. Munro, V. Christensen, and D. Pauly, editors. Assessment, management, and future directions for coastal fisheries in asian countries. Book Section, WorldFish Center Conference Proceedings 67, WorldFish Center, Penang.

Wood, S. N. 2011. Fast stable restricted maximum likelihood and marginal likelihood estimation of semiparametric generalized linear models. Journal of the Royal Statistical Society B 73:3–36.

Wood, S. N. 2017. Generalized additive models: An introduction with r. 2nd editions.

Book, Chapman; Hall/CRC.

Wood, S. N., N. Pya, and B. Safken. 2016. Smoothing parameter and model selection for general smooth models (with discussion). Journal of the American Statistical Association 111:1548–1575.

1972.. Chart or Table.

2016.. Personal Communication.

2017, 11-03-2017.. Online Database.

Figure Legends

Figure 1. Close up of Kerala State with the latitude/longitude boxes used for the satellite data. Kerala State is marked in grey and the oil sardine catch from this region is being modeled.

Figure 2. Quarterly catch data 1956-2014 from Kerala. The catches have a strong seasonal pattern with the highest catches in quarter 4 Note that quarter 3 is July-Sept and that the fishery is closed July 1 to Aug 15, thus the fishery is only open 1.5 months in quarter 3. The mean catch (metric tonnes) in quarters 1 to 4 are 38, 19.2, 30.9, and 59.9 metric tonnes respectively.

Figure 5. Cartoon of the sardine life-cycle in the SE Indian Ocean and how it interacts with the fishery.

Figure 6. Remote sensing covariates used in the analysis. All data are monthly averages over Box 4 in Figure 1 on the Kerala coast off of Kochi. Panel A) Upwelling Index. The upwelling index is the difference between the near-shore sea surface temperature (SST) and the off-shore SST defined as 3 degrees longitude offshore. Panel B) Surface chlorophyll-a (Chl-a). The Chl-a data are only available from 1997 onward. Panel C) Sea surface temperature constructed from Advanced Very High Resolution Radiometer (AVHRR). Panel D) Average daily rainfall (mm/day) off the Kerala coast.

Figure 7. Key oil sardine life-history events overlaid on the monthly SST in the near-shore and off-shore and the near-shore Chl-a.

Figure 3. Effects of covariates estimated from the GAM models. Panel A) Effect of SST during the spawning months (Jul-Sep) on catch during the spawning months. Low SST is associated with lower that expected catch during the spawning months. Panel B) Effect of upwelling (inshore/off-shore SST differential) during Jan-Mar of the prior season on catch during the next spawning months (Jul-Sep). The index is the difference between offshore and inshore SST, thus a negative value indicates warmer coastal surface water than off-shore. Warm coastal water during Jan-Mar when sardines are foraging along the coast, is associated with lower catch during the next spawning season. Panel C) Effect of SST during the spawning months (Jul-Sep) on catch during the subsequent non-spawning months (Oct-Jun). Low SST is associated with lower that expected catch during the following non-spawning months. Panel D) Effect of upwelling (inshore/off-shore SST differential) during Oct-Dec of the prior season on catch during the non-spawning months (Oct-Jun) the next season. Strong upwelling (positive upwelling index) in the early larval and juvenile period (Oct-Dec) is associated with higher than expected catch in the next season.

Figure 8. Fitted versus observed catch with models with and without environmental covariates. Panel A) Fitted versus observed log catch in the spawning months with only non-spawning catch in the previous season as the covariate: $S_t = s(N_{t-1}) + \varepsilon$. Panel B) Fitted versus observed log catch in the spawning months with Jan-Mar upwelling in the prior season added as a covariate to the model: $s(V_{t-1})$. Panel C) Fitted versus observed log catch in the non-spawning months with only non-spawning catch in the previous season and spawning catch two season prior as the covariates: $N_t = s(N_{t-1}) + s(S_{t-2}) + \varepsilon$. Panel D) Fitted versus observed log catch in the non-spawning months with current season SST in Jul-Sep (V) and Oct-Dec upwelling in the prior season (W) added as covariates: $s(V_t) + \beta W_{t-1}$. W was added linearly since the data were insufficient to estimate four non-linear effects.

Table 1. Model selection tests of time-dependency and linearity for the S_t model using F-tests of nested models fit to log landings data. S_t is the catch during the spawning period (Qtr 3 = July-Sep) of season t (Jul-Jun). N_{t-1} is the catch during the prior sardine season after the spawning period (the 9-months following Qtr 3, Oct-Jun, of the previous sardine season). N_{t-2} is the same for two seasons prior. $s()$ is a non-linear function of the response variable.

Model	Residual df	Residual deviance	F	p value	AIC
Time dependency test 1982-2015 data					
$ln(S_t) = \alpha + \varepsilon$	33	65.13			122.59
(Var(ε) = 1.97)					
$ln(S_t) = \alpha + \beta ln(N_{t-1}) + \varepsilon$	32	48.37	10.85	0.002	114.47
($R^2 adj$ = 23%, Var(ε) = 1.51)					
$ln(S_t) = \alpha + \beta_1 ln(N_{t-1}) + \beta_2 ln(N_{t-2}) + \varepsilon$	31	48.18	0.12	0.729	116.34
($R^2 adj$ = 21%, Var(ε) = 1.55)					
Linearity test 1982-2015 data					
$ln(S_t) = \alpha + \beta ln(N_{t-1}) + \varepsilon$	32	48.37			114.47
($R^2 adj$ = 23%, Var(ε) = 1.51)					
$ln(S_t) = \alpha + s(ln(N_{t-1})) + \varepsilon$	30.6	44.8	1.74	0.199	113.76
($R^2 adj$ = 27%, Var(ε) = 1.44)					
$ln(S_t) = \alpha + s(ln(N_{t-1})) + s(ln(N_{t-2})) + \varepsilon$	28.2	42.91	0.54	0.618	116.14
($R^2 adj$ = 25%, Var(ε) = 1.47)					
$ln(S_t) = \alpha + s(ln(N_{t-1})) + s(ln(S_{t-2})) + \varepsilon$	27.7	40.87	0.97	0.419	115.33
($R^2 adj$ = 28%, Var(ε) = 1.42)					

Table 2. Model selection tests for the N_t model using AIC for models fit to log landings data. S_t is the catch during the spawning season. N_t is the catch during the non-spawning period (Qtrs 4, 1 and 2: Oct-Jun) of season t (Jul-Jun). S_{t-1} and N_{t-1} are the catch during the prior sardine season during and after the spawning period respectively. S_{t-2} and N_{t-2} are the same for two seasons prior.

Model	Residual df	Residual deviance	F	p value	AIC
$ln(N_t) = \alpha + \beta ln(N_{t-1}) + \varepsilon$ ($R^2 adj = 39\%$, Var(ε) = 0.88)	31	27.42			93.54
$ln(N_t) = \alpha + s(ln(N_{t-1})) + \varepsilon$ ($R^2 adj = 47\%$, Var(ε) = 0.77)	29.5	23.04	5.2	0.02	89.79
$ln(N_t) = \alpha + s_1(ln(N_{t-1})) + s_2(ln(N_{t-2})) + \varepsilon$ ($R^2 adj = 51\%$, Var(ε) = 0.71)	27.2	19.95	2.28	0.115	88.81
$ln(N_t) = \alpha + s_1(ln(N_{t-1})) + s_2(ln(S_{t-2})) + \varepsilon$ ($R^2 adj = 60\%$, Var(ε) = 0.58)	26.5	15.97	10	0.008	82.62

Table 3. Top covariates for the spawner (S_t) and non-spawner (N_t) models. The models are nested; the roman numeral indicates the level of nestedness. Models at levels II and higher are shown with the component that is added to the base level model (M0 or M1) at top. The full set of covariate models tested are given in Appendix B. The fitted versus observed catches from the covariate models are shown in Figure 8.

Model	Residual df	Residual deviance	F	p value	AIC
Spawner catch models with covariates					
V_t = Jul-Sep SST current season					
W_{t-1} = Jan-Mar upwelling prior season					
I-M0: $ln(S_t) = \alpha + s(ln(N_{t-1})) + \varepsilon$	29.6	44.66			111.57
($R^2 adj$ = 27%, Var(ε) = 1.49)					
II: $ln(S_t) = M0 + s(V_t)$	27	35.62	2.73	0.073	108.26
($R^2 adj$ = 37%, Var(ε) = 1.27)					
III: $ln(S_t) = M0 + s(V_t) + s(W_{t-1})$	24.4	33.06	0.76	0.514	110.1
($R^2 adj$ = 37%, Var(ε) = 1.28)					
II: $ln(S_t) = M0 + s(W_{t-1})$	26.9	42.45	0.53	0.648	114.3
($R^2 adj$ = 25%, Var(ε) = 1.53)					
Spawner catch models with covariates					
V_t = Jul-Sep SST current season					
W_{t-1} = Oct-Dec upwelling prior season					
I-M1: $ln(N_t) = \alpha + s(ln(N_{t-1})) + s(ln(S_{t-2})) + \varepsilon$	25.6	15.58			80.66
($R^2 adj$ = 61%, Var(ε) = 0.59)					
II: $ln(N_t) = M1 + s(V_t)$	23.1	9.78	5.8	0.007	69.77
($R^2 adj$ = 73%, Var(ε) = 0.4)					
III: $ln(N_t) = M1 + s(V_t) + \beta W_{t-1}$	22.1	9.61	0.44	0.505	71.14
($R^2 adj$ = 73%, Var(ε) = 0.41)					
II: $ln(N_t) = M1 + s(W_{t-1})$	23.3	14.94	0.48	0.649	82.97
($R^2 adj$ = 59%, Var(ε) = 0.6)					

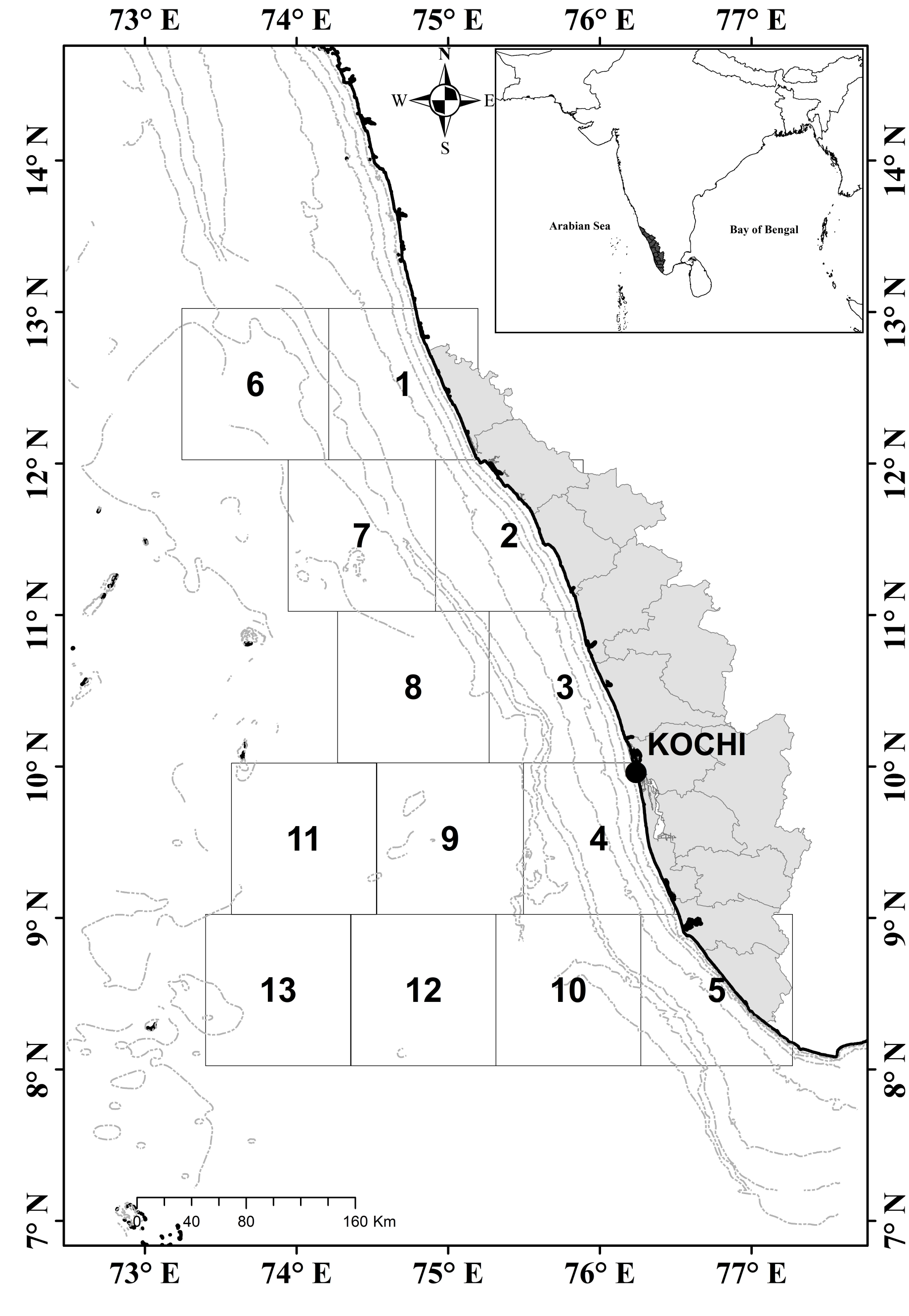

73° E
74° E
75° E
76° E
77° E
14° N
13° N
12° N
11° N
10° N
9° N
8° N
7° N
N
W
E
S
Arabian Sea
Bay of Bengal
1
2
3
4
5
6
7
8
9
10
11
12
13
KOCHI
0
40
80
160 Km

Figure 1

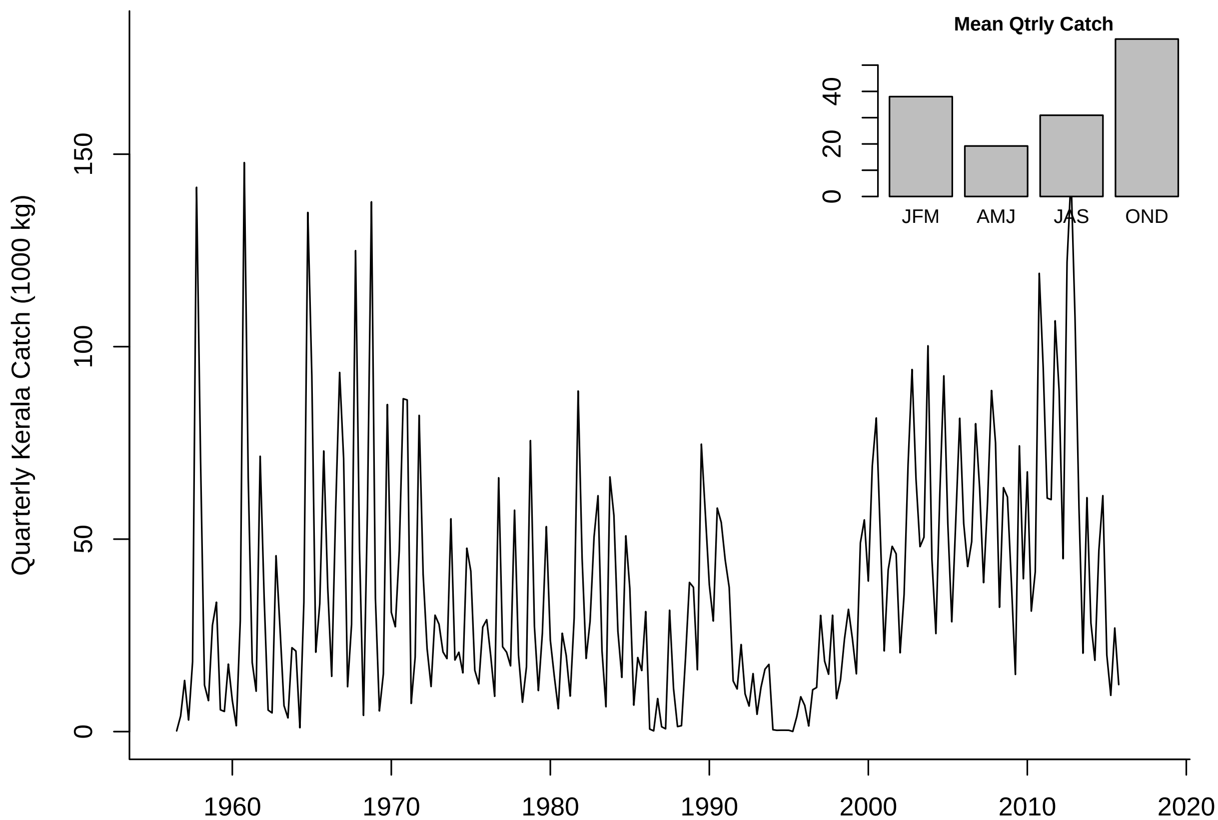
Mean Qtrly Catch
0
20
40
JFM
AMJ
JAS
OND
Quarterly Kerala Catch (1000 kg)
0
50
100
150
1960
1970
1980
1990
2000
2010
2020

Figure 2

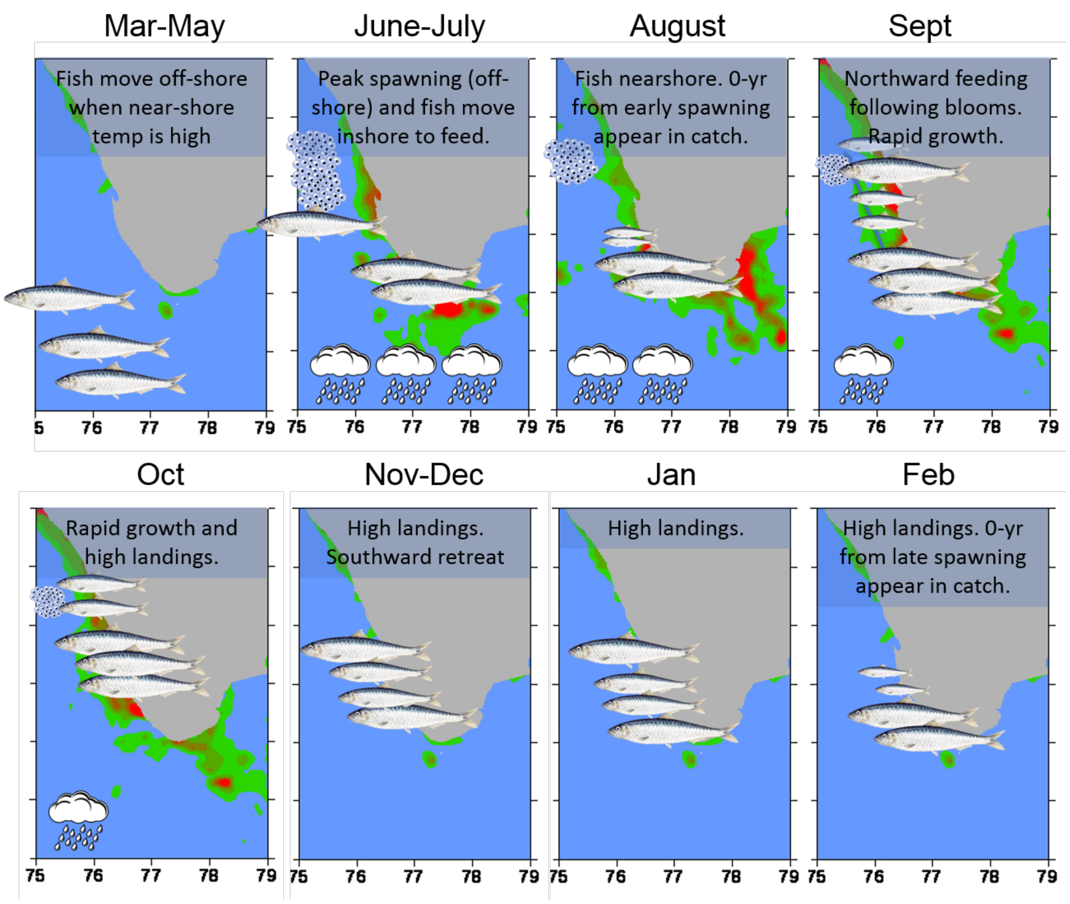
Mar-May
Fish move off-shore when near-shore temp is high
June-July
Peak spawning (off-shore) and fish move inshore to feed.
August
Fish nearshore. 0-yr from early spawning appear in catch.
Sept
Northward feeding following blooms. Rapid growth.
Oct
Rapid growth and high landings.
Nov-Dec
High landings. Southward retreat
Jan
High landings.
Feb
High landings. 0-yr from late spawning appear in catch.
75
76
77
78
79

Figure 5

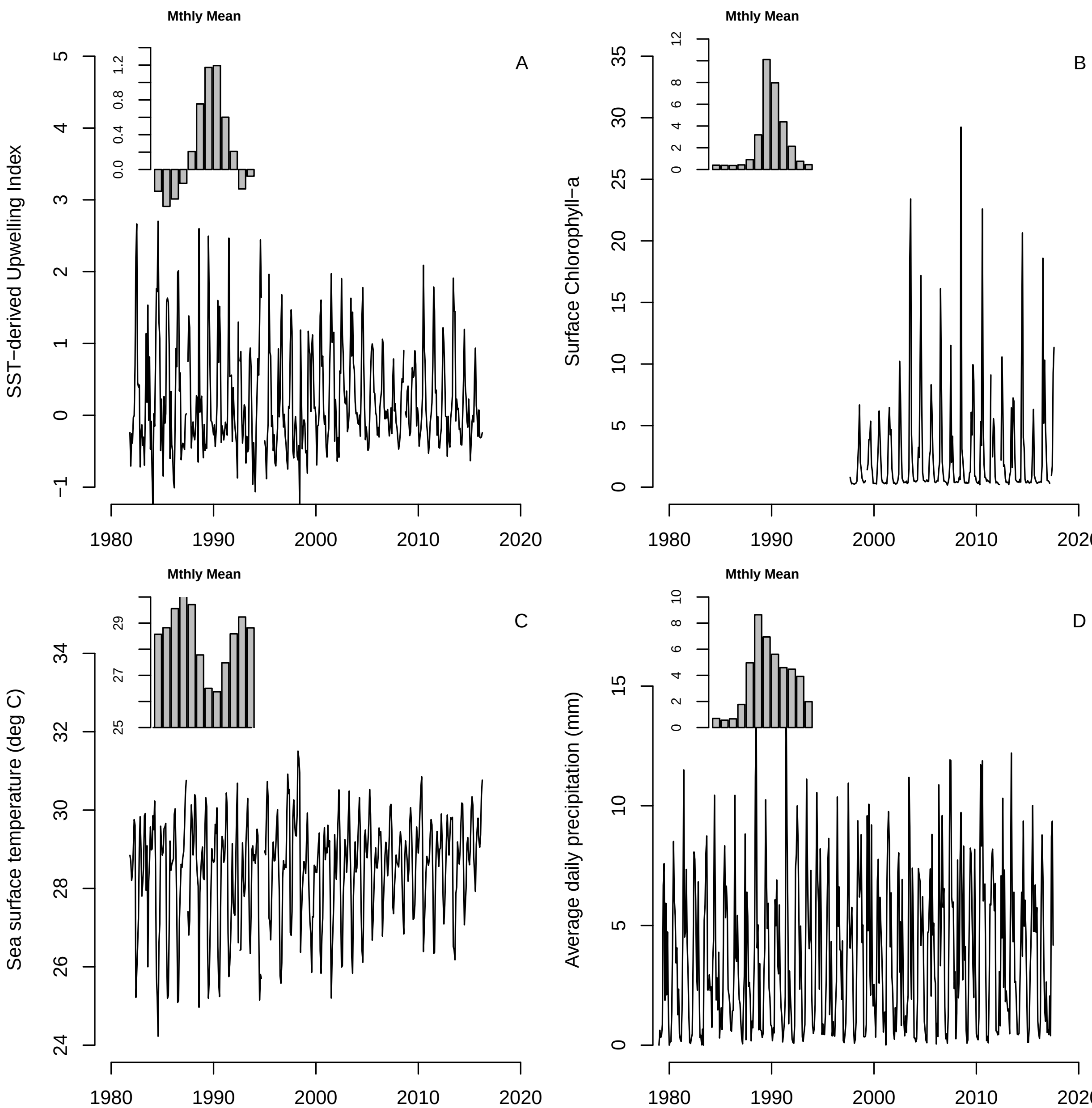

Mthly Mean
A
SST−derived Upwelling Index
Mthly Mean
B
Surface Chlorophyll−a
Mthly Mean
C
Sea surface temperature (deg C)
Mthly Mean
D
Average daily precipitation (mm)
1980
1990
2000
2010
2020

Figure 6

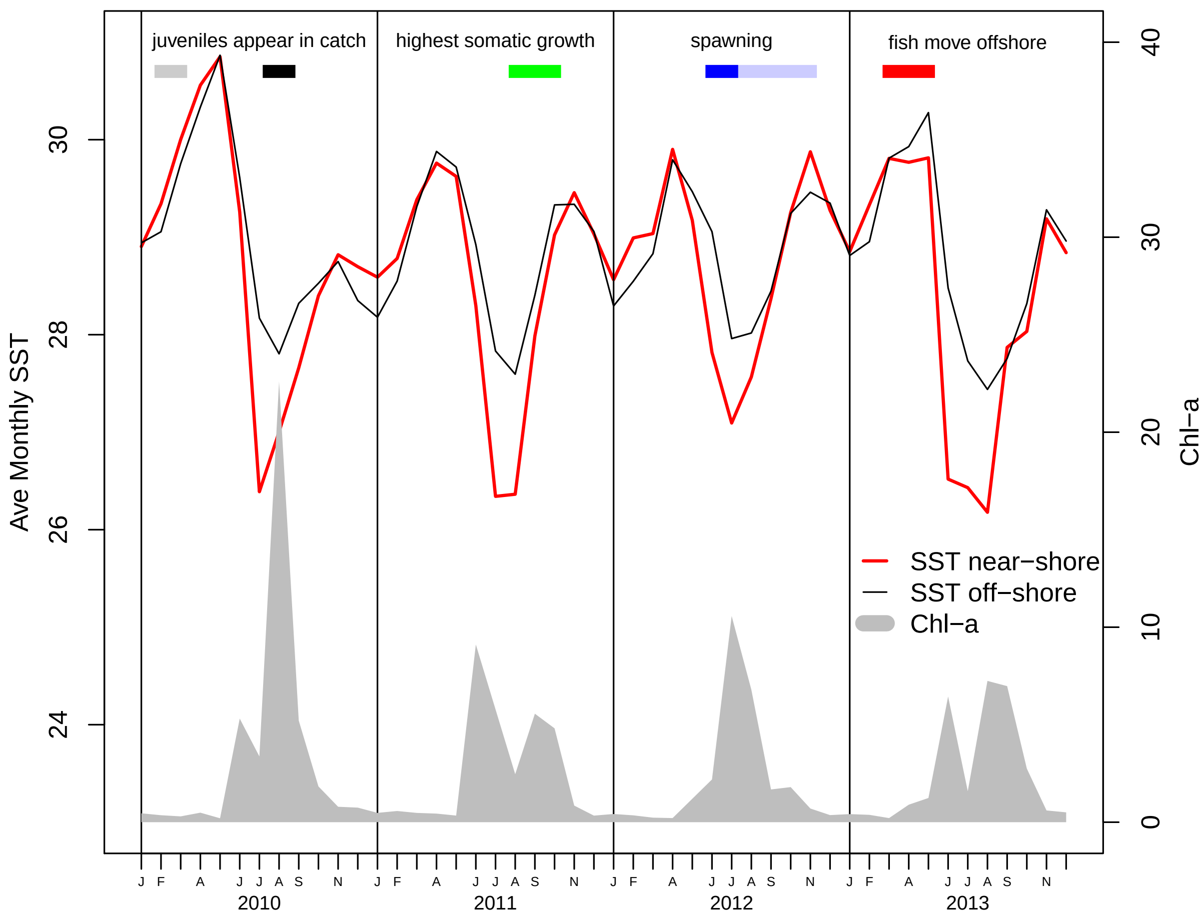
juveniles appear in catch
highest somatic growth
spawning
fish move offshore
Ave Monthly SST
Chl−a
SST near−shore
SST off−shore
Chl−a
2010
2011
2012
2013

Figure 7

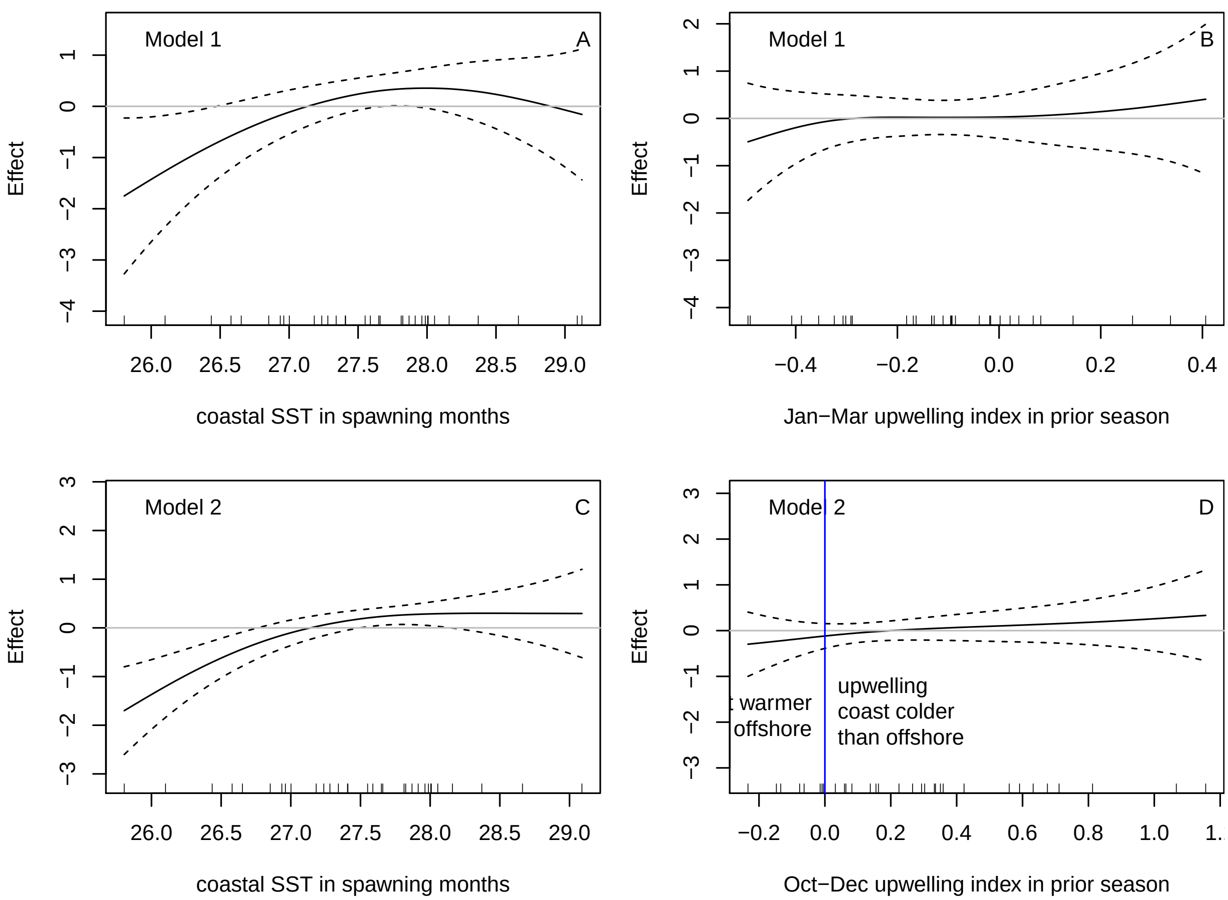
Model 1
A
Effect
coastal SST in spawning months
Model 1
B
Effect
Jan−Mar upwelling index in prior season
Model 2
C
Effect
coastal SST in spawning months
Model 2
D
Effect
t warmer
offshore
upwelling
coast colder
than offshore
Oct−Dec upwelling index in prior season

Figure 3

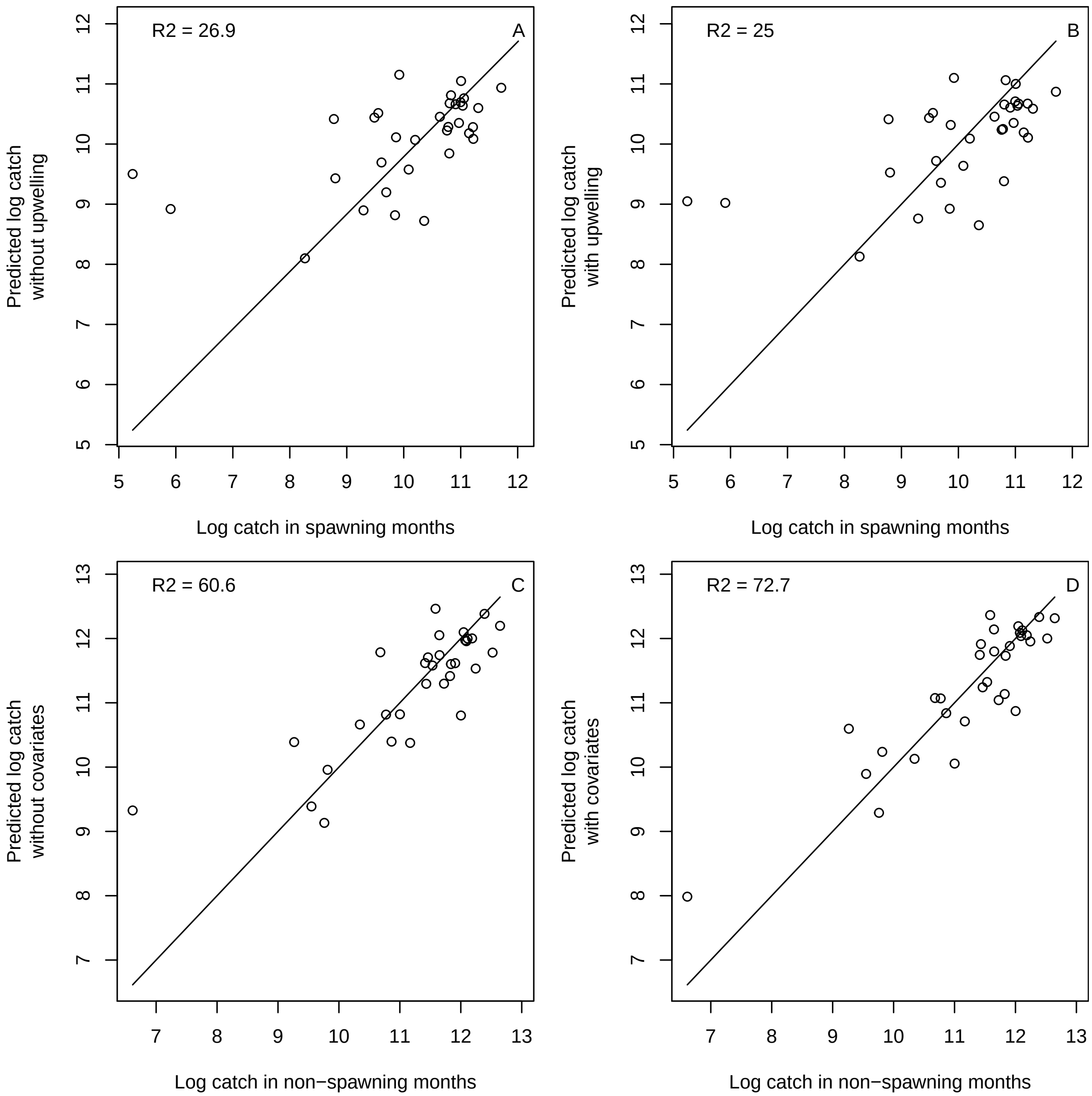
R2 = 26.9
A
Predicted log catch without upwelling
Log catch in spawning months
R2 = 25
B
Predicted log catch with upwelling
Log catch in spawning months
R2 = 60.6
C
Predicted log catch without covariates
Log catch in non−spawning months
R2 = 72.7
D
Predicted log catch with covariates
Log catch in non−spawning months

Figure 8

Appendices

Appendix A: Tests for prior season catch as covariate

Table A1. Model selection tests of time-dependency the log catch during spawning months using F-tests of nested linear models. S_t is the catch during the spawning period (Jul-Sep). N_t is the catch during the non-spawning period (Oct-Jun). S_{t-1} and N_{t-1} are the catch during the prior season during and after the spawning period respectively. S_{t-2} and N_{t-2} are the same for two seasons prior. Test A uses catch during the spawning period as the explanatory variable. Test B uses catch during the non-spawning period as the explanatory variable. Test C uses both. For Test C, the nestedness is lines 1-3 and lines 1-2 and 4.

Model	Residual df	Residual deviance	F	p value	AIC
Time dependency test A 1983-2015 data					
$ln(S_t) = \alpha + \varepsilon$	32	65.09			120.07
(Var(ε) = 2.03)					
$ln(S_t) = \alpha + \beta ln(S_{t-1}) + \varepsilon$	31	56.91	4.61	0.04	117.63
($R^2 adj$ = 10%, Var(ε) = 1.84)					
$ln(S_t) = \alpha + \beta_1 ln(S_{t-1}) + \beta_2 ln(S_{t-2}) + \varepsilon$	30	53.27	2.05	0.163	117.45
($R^2 adj$ = 13%, Var(ε) = 1.78)					
Time dependency test B 1983-2015 data					
$ln(S_t) = \alpha + \varepsilon$	32	65.09			120.07
(Var(ε) = 2.03)					
$ln(S_t) = \alpha + \beta ln(N_{t-1}) + \varepsilon$	31	48.33	10.45	0.003	112.24
($R^2 adj$ = 23%, Var(ε) = 1.56)					
$ln(S_t) = \alpha + \beta_1 ln(N_{t-1}) + \beta_2 ln(N_{t-2}) + \varepsilon$	30	48.11	0.14	0.714	114.09
($R^2 adj$ = 21%, Var(ε) = 1.6)					
Time dependency test C 1983-2015 data					
$ln(S_t) = \alpha + \beta ln(N_{t-1}) + \varepsilon$	31	48.33			112.24
($R^2 adj$ = 23%, Var(ε) = 1.56)					
$ln(S_t) = \alpha + \beta_1 ln(N_{t-1}) + \beta_2 ln(S_{t-1}) + \varepsilon$	30	47.65	0.43	0.517	113.77
($R^2 adj$ = 22%, Var(ε) = 1.59)					
$ln(S_t) = \alpha + \beta_1 ln(N_{t-1}) + \beta_2 ln(S_{t-2}) + \varepsilon$	30	47.89	0.28	0.601	113.94
($R^2 adj$ = 22%, Var(ε) = 1.6)					

Table A2. Model selection tests of time-dependency the catch during spawning months using non-linear responses instead of linear responses as in Table A1 See Table A1 for an explanation of the parameters and model set-up.

Model	Residual df	Residual deviance	F	p value	AIC
Time dependency test A 1983-2015 data					
$ln(S_t) = \alpha + \beta ln(S_{t-1}) + \varepsilon$ ($R^2 adj = 10\%$, Var(ε) = 1.84)	31	56.91			117.63
$ln(S_t) = \alpha + s(ln(S_{t-1})) + \varepsilon$ ($R^2 adj = 20\%$, Var(ε) = 1.63)	29	48.2	2.73	0.085	115.01
$ln(S_t) = \alpha + s_1(ln(S_{t-1})) + s_2(ln(S_{t-2})) + \varepsilon$ ($R^2 adj = 20\%$, Var(ε) = 1.62)	26.2	44.27	0.86	0.466	116.82
Time dependency test B 1983-2015 data					
$ln(S_t) = \alpha + \beta ln(N_{t-1}) + \varepsilon$ ($R^2 adj = 23\%$, Var(ε) = 1.56)	31	48.33			112.24
$ln(S_t) = \alpha + s(ln(N_{t-1})) + \varepsilon$ ($R^2 adj = 27\%$, Var(ε) = 1.49)	29.6	44.66	1.71	0.203	111.57
$ln(S_t) = \alpha + s_1(ln(N_{t-1})) + s_2(ln(N_{t-2})) + \varepsilon$ ($R^2 adj = 26\%$, Var(ε) = 1.51)	27.3	42.64	0.57	0.594	113.79
Time dependency test C 1983-2015 data					
$ln(S_t) = \alpha + s(ln(N_{t-1})) + \varepsilon$ ($R^2 adj = 27\%$, Var(ε) = 1.49)	29.6	44.66			111.57
$ln(S_t) = \alpha + s_1(ln(N_{t-1})) + s_2(ln(S_{t-1})) + \varepsilon$ ($R^2 adj = 32\%$, Var(ε) = 1.39)	26.9	38.53	1.66	0.202	111.12
$ln(S_t) = \alpha + s_1(ln(N_{t-1})) + s_2(ln(S_{t-2})) + \varepsilon$ ($R^2 adj = 28\%$, Var(ε) = 1.47)	26.8	40.64	0.98	0.414	113.05

Table A3. Model selection tests of time-dependency for the catch during spawning months using 1956-2015 data. See Table A1 for definitions.

Model	Residual df	Residual deviance	F	p value	AIC
Time dependency test B linear 1956-2015 data					
$ln(S_t) = \alpha + \varepsilon$	57	80.84			187.85
($R^2 adj = 0\%$, Var(ε) = 1.42)					
$ln(S_t) = \alpha + \beta ln(N_{t-1}) + \varepsilon$	56	67.58	10.79	0.002	179.46
($R^2 adj = 15\%$, Var(ε) = 1.21)					
$ln(S_t) = \alpha + \beta_1 ln(N_{t-1}) + \beta_2 ln(N_{t-2}) + \varepsilon$	55	67.58	0	0.97	181.46
($R^2 adj = 13\%$, Var(ε) = 1.23)					
Linearity test 1956-2015 data					
$ln(S_t) = \alpha + \beta ln(N_{t-1}) + \varepsilon$	56	67.58			179.46
($R^2 adj = 15\%$, Var(ε) = 1.21)					
$ln(S_t) = \alpha + s(ln(N_{t-1})) + \varepsilon$	54.6	65.7	1.13	0.312	179.64
($R^2 adj = 16\%$, Var(ε) = 1.19)					
$ln(S_t) = \alpha + s_1(ln(N_{t-1})) + s_2(ln(N_{t-2})) + \varepsilon$	52.3	65	0.25	0.811	182.78
($R^2 adj = 14\%$, Var(ε) = 1.22)					

Table A4. Model selection tests of time-dependency the N_t model using F-tests of nested models fit to 1983 to 2014 log landings data. The years are determined by the covariate data availability. N_t is the catch during the non-spawning period (Qtrs 4, 1 and 2: Oct-Jun) of season t (Jul-Jun). S_{t-1} and N_{t-1} are the catch during the prior sardine season during and after the spawning period respectively. S_{t-2} and N_{t-2} are the same for two seasons prior. Test A uses catch during the spawning period as the explanatory variable. Test B uses catch during the non-spawning period as the explanatory variable. Test C uses both. For Test C, the nestedness is lines 1-3 and lines 1-2 and 4.

Model	Residual df	Residual deviance	F	p value	AIC
Time dependency test A 1983-2014 data					
$ln(N_t) = \alpha + \varepsilon$	31	46.19			106.56
(Var(ε) = 1.49)					
$ln(N_t) = \alpha + \beta ln(S_{t-1}) + \varepsilon$	30	32.39	12.77	0.001	97.2
(R^2adj = 28%, Var(ε) = 1.08)					
$ln(N_t) = \alpha + \beta_1 ln(S_{t-1}) + \beta_2 ln(S_{t-2}) + \varepsilon$	29	31.31	1	0.325	98.12
(R^2adj = 28%, Var(ε) = 1.08)					
Time dependency test B 1983-2014 data					
$ln(N_t) = \alpha + \varepsilon$	31	46.19			106.56
(Var(ε) = 1.49)					
$ln(N_t) = \alpha + \beta ln(N_{t-1}) + \varepsilon$	30	27.41	20.17	0	91.85
(R^2adj = 39%, Var(ε) = 0.91)					
$ln(N_t) = \alpha + \beta_1 ln(N_{t-1}) + \beta_2 ln(N_{t-2}) + \varepsilon$	29	27	0.43	0.517	93.38
(R^2adj = 38%, Var(ε) = 0.93)					
Time dependency test C 1983-2014 data					
$ln(N_t) = \alpha + \beta ln(N_{t-1}) + \varepsilon$	30	27.41			91.85
(R^2adj = 39%, Var(ε) = 0.91)					
$ln(N_t) = \alpha + \beta_1 ln(N_{t-1}) + \beta_2 ln(S_{t-1}) + \varepsilon$	29	27.32	0.1	0.759	93.75
(R^2adj = 37%, Var(ε) = 0.94)					
$ln(N_t) = \alpha + \beta_1 ln(N_{t-1}) + \beta_2 ln(S_{t-2}) + \varepsilon$	29	27.4	0.01	0.93	93.84
(R^2adj = 37%, Var(ε) = 0.94)					

Table A5. Model selection tests of time-dependency the N_t model using non-linear responses instead of linear responses as in Table A4 See Table A4 for an explanation of the parameters and model set-up.

Model	Residual df	Residual deviance	F	p value	AIC
Time dependency test A 1983-2014 data					
$ln(N_t) = \alpha + \beta ln(S_{t-1}) + \varepsilon$ ($R^2 adj = 28\%$, Var(ε) = 1.08)	30	32.39			97.2
$ln(N_t) = \alpha + s(ln(S_{t-1})) + \varepsilon$ ($R^2 adj = 31\%$, Var(ε) = 1.03)	28.1	29.4	1.68	0.207	96.88
$ln(N_t) = \alpha + s_1(ln(S_{t-1})) + s_2(ln(S_{t-2})) + \varepsilon$ ($R^2 adj = 38\%$, Var(ε) = 0.93)	25.1	24.35	1.84	0.166	95.69
Time dependency test B 1983-2014 data					
$ln(N_t) = \alpha + \beta ln(N_{t-1}) + \varepsilon$ ($R^2 adj = 39\%$, Var(ε) = 0.91)	30	27.41			91.85
$ln(N_t) = \alpha + s(ln(N_{t-1})) + \varepsilon$ ($R^2 adj = 47\%$, Var(ε) = 0.79)	28.5	22.99	4.07	0.04	88.28
$ln(N_t) = \alpha + s_1(ln(N_{t-1})) + s_2(ln(N_{t-2})) + \varepsilon$ ($R^2 adj = 51\%$, Var(ε) = 0.73)	26.3	19.89	1.87	0.171	87.3
Time dependency test C 1983-2014 data					
$ln(N_t) = \alpha + s(ln(N_{t-1})) + \varepsilon$ ($R^2 adj = 47\%$, Var(ε) = 0.79)	28.5	22.99			88.28
$ln(N_t) = \alpha + s_1(ln(N_{t-1})) + s_2(ln(S_{t-1})) + \varepsilon$ ($R^2 adj = 45\%$, Var(ε) = 0.81)	25.9	21.83	0.55	0.631	90.96
$ln(N_t) = \alpha + s_1(ln(N_{t-1})) + s_2(ln(S_{t-2})) + \varepsilon$ ($R^2 adj = 61\%$, Var(ε) = 0.59)	25.6	15.58	4.26	0.015	80.66

Table A6. Table A5 with 1956-2015 data instead of 1983 to 2014 data. See Table A4 for an explanation of the parameters and model set-up.

Model	Residual df	Residual deviance	F	p value	AIC
Time dependency test A 1956-2015 data					
$ln(N_t) = \alpha + \beta ln(S_{t-1}) + \varepsilon$	55	43.02			151.71
($R^2 adj$ = 19%, Var(ε) = 0.78)					
$ln(N_t) = \alpha + s(ln(S_{t-1})) + \varepsilon$	53.4	41.68	1.04	0.348	152.24
($R^2 adj$ = 20%, Var(ε) = 0.77)					
$ln(N_t) = \alpha + s_1(ln(S_{t-1})) + s_2(ln(S_{t-2})) + \varepsilon$	50.7	40.21	0.71	0.534	154.53
($R^2 adj$ = 20%, Var(ε) = 0.78)					
Time dependency test B 1956-2015 data					
$ln(N_t) = \alpha + \beta ln(N_{t-1}) + \varepsilon$	55	36.81			142.84
($R^2 adj$ = 31%, Var(ε) = 0.67)					
$ln(N_t) = \alpha + s(ln(N_{t-1})) + \varepsilon$	53.6	35.24	1.75	0.191	142.2
($R^2 adj$ = 33%, Var(ε) = 0.65)					
$ln(N_t) = \alpha + s_1(ln(N_{t-1})) + s_2(ln(N_{t-2})) + \varepsilon$	51.3	33.96	0.87	0.439	143.8
($R^2 adj$ = 33%, Var(ε) = 0.65)					
Time dependency test C 1956-2015 data					
$ln(N_t) = \alpha + s(ln(N_{t-1})) + \varepsilon$	53.6	35.24			142.2
($R^2 adj$ = 33%, Var(ε) = 0.65)					
$ln(N_t) = \alpha + s_1(ln(N_{t-1})) + s_2(ln(S_{t-1})) + \varepsilon$	51.2	33.5	1.12	0.342	143.28
($R^2 adj$ = 34%, Var(ε) = 0.64)					
$ln(N_t) = \alpha + s_1(ln(N_{t-1})) + s_2(ln(S_{t-2})) + \varepsilon$	51	33.97	0.75	0.513	144.43
($R^2 adj$ = 32%, Var(ε) = 0.65)					

Table A7. Model selection tests for the N_t model using AIC for models fit to log landings data with catch during the spawning season S_t added as a covariate. Data 1983 to 2014 were used.

Model	Residual df	Residual deviance	AIC
Add current season spawning information			
$ln(N_t) = \alpha + \beta ln(S_t) + \varepsilon$	30	15.41	73.43
($R^2 adj$ = 66%, Var(ε) = 0.51)			
$ln(N_t) = \alpha + s(ln(S_t)) + \varepsilon$	28.2	14.79	74.64
($R^2 adj$ = 65%, Var(ε) = 0.51)			
$ln(N_t) = \alpha + \beta ln(S_t) + s(ln(S_{t-1})) + \varepsilon$	27.1	11.51	68.8
($R^2 adj$ = 72%, Var(ε) = 0.42)			
$ln(N_t) = \alpha + \beta ln(S_t) + s(ln(N_{t-1})) + \varepsilon$	27.5	10.93	66.45
($R^2 adj$ = 74%, Var(ε) = 0.39)			

Appendix B: Tests for environmental variables as covariates

Table B1. Model selection tests of GPCP precipitation as an explanatory variable for the catch during spawning months (Jul-Sep) using 1983 to 2015 data. The data range is determined by the years for which SST was available in order to use a consistent dataset across covariate tests. S_t is the catch during Jul-Sep of season t. V_t is the covariate in the current season which spans two calendar years from July to June in the next year. V_{t-1} is the covariate in the prior Jul-Jun season.

Model	Residual df	Residual deviance	F	p value	AIC
V = Jun-Jul Precipitation					
$ln(S_t) = \alpha + s(ln(N_{t-1})) + \varepsilon$	29.6	44.66			111.57
(R^2adj = 27%, Var(ε) = 1.49)					
$ln(S_t) = \alpha + s(ln(N_{t-1})) + \beta V_t + \varepsilon$	28.6	43.39	0.86	0.361	112.56
(R^2adj = 27%, Var(ε) = 1.49)					
$ln(S_t) = \alpha + s(ln(N_{t-1})) + s(V_t) + \varepsilon$	26.8	40.45	1.08	0.348	112.74
(R^2adj = 29%, Var(ε) = 1.45)					
$ln(S_t) = \alpha + s(ln(N_{t-1})) + s(V_t) + \beta V_{t-1} + \varepsilon$	25.9	39.91	0.37	0.543	114.23
(R^2adj = 27%, Var(ε) = 1.49)					
$ln(S_t) = \alpha + s(ln(N_{t-1})) + s(V_t) + s(V_{t-1}) + \varepsilon$	24.2	39.13	0.3	0.707	115.94
(R^2adj = 25%, Var(ε) = 1.52)					
V = Apr-May Precipitation					
$ln(S_t) = \alpha + s(ln(N_{t-1})) + \varepsilon$	29.6	44.66			111.57
(R^2adj = 27%, Var(ε) = 1.49)					
$ln(S_t) = \alpha + s(ln(N_{t-1})) + \beta V_t + \varepsilon$	28.6	43.46	0.78	0.386	112.65
(R^2adj = 26%, Var(ε) = 1.5)					
$ln(S_t) = \alpha + s(ln(N_{t-1})) + s(V_t) + \varepsilon$	26.8	42.17	0.45	0.621	114.13
(R^2adj = 25%, Var(ε) = 1.52)					
$ln(S_t) = \alpha + s(ln(N_{t-1})) + s(V_t) + \beta V_{t-1} + \varepsilon$	25.8	42.18	NA	NA	116.09
(R^2adj = 23%, Var(ε) = 1.57)					
$ln(S_t) = \alpha + s(ln(N_{t-1})) + s(V_t) + s(V_{t-1}) + \varepsilon$	24.1	40.14	0.76	0.459	116.79
(R^2adj = 23%, Var(ε) = 1.56)					

Table B3. Model selection tests of sea surface temperature off Cochi as the explanatory variable (V) for the catch during spawning months (Jul-Sep) using 1983 to 2015 data. See Table B1 for an explanation of the models.

Model	Residual df	Residual deviance	F	p value	AIC
V = Jul-Sep SST					
$ln(S_t) = \alpha + s(ln(N_{t-1})) + \varepsilon$	29.6	44.66			111.57
($R^2 adj$ = 27%, Var(ε) = 1.49)					
$ln(S_t) = \alpha + s(ln(N_{t-1})) + \beta V_t + \varepsilon$	28.6	42.38	1.86	0.184	111.77
($R^2 adj$ = 28%, Var(ε) = 1.46)					
$ln(S_t) = \alpha + s(ln(N_{t-1})) + s(V_t) + \varepsilon$	27	35.62	3.35	0.061	108.26
($R^2 adj$ = 37%, Var(ε) = 1.27)					
$ln(S_t) = \alpha + s(ln(N_{t-1})) + s(V_t) + \beta V_{t-1} + \varepsilon$	26	34.03	1.34	0.256	108.68
($R^2 adj$ = 38%, Var(ε) = 1.26)					
$ln(S_t) = \alpha + s(ln(N_{t-1})) + s(V_t) + s(V_{t-1}) + \varepsilon$	24.7	32.65	0.79	0.422	109.19
($R^2 adj$ = 38%, Var(ε) = 1.25)					
V = Jan-Dec SST					
$ln(S_t) = \alpha + s(ln(N_{t-1})) + \varepsilon$	29.6	44.66			111.57
($R^2 adj$ = 27%, Var(ε) = 1.49)					
$ln(S_t) = \alpha + s(ln(N_{t-1})) + \beta V_t + \varepsilon$	28.6	41.84	1.98	0.172	111.38
($R^2 adj$ = 29%, Var(ε) = 1.44)					
$ln(S_t) = \alpha + s(ln(N_{t-1})) + s(V_t) + \varepsilon$	26.7	41.56	0.1	0.9	113.89
($R^2 adj$ = 26%, Var(ε) = 1.5)					
$ln(S_t) = \alpha + s(ln(N_{t-1})) + s(V_t) + \beta V_{t-1} + \varepsilon$	25.7	39.4	1.58	0.22	114.02
($R^2 adj$ = 28%, Var(ε) = 1.47)					
$ln(S_t) = \alpha + s(ln(N_{t-1})) + s(V_t) + s(V_{t-1}) + \varepsilon$	23.9	37.02	0.91	0.406	114.58
($R^2 adj$ = 28%, Var(ε) = 1.46)					

Table B4. Model selection tests of upwelling intensity off Cochi as the explanatory variable. See Table B1 for an explanation of the models.

Model	Residual df	Residual deviance	F	p value	AIC
V = Jul-Sep Upwelling current and prior seasons					
$ln(S_t) = \alpha + s(ln(N_{t-1})) + \varepsilon$	29.6	44.66			111.57
($R^2adj = 27\%$, Var(ε) = 1.49)					
$ln(S_t) = \alpha + s(ln(N_{t-1})) + \beta V_t + \varepsilon$	28.6	40.75	2.63	0.119	110.5
($R^2adj = 31\%$, Var(ε) = 1.4)					
$ln(S_t) = \alpha + s(ln(N_{t-1})) + s(V_t) + \varepsilon$	26.6	39.74	0.34	0.712	112.5
($R^2adj = 29\%$, Var(ε) = 1.44)					
$ln(S_t) = \alpha + s(ln(N_{t-1})) + s(V_t) + \beta V_{t-1} + \varepsilon$	25.7	39.71	0.02	0.886	114.38
($R^2adj = 27\%$, Var(ε) = 1.49)					
$ln(S_t) = \alpha + s(ln(N_{t-1})) + s(V_t) + s(V_{t-1}) + \varepsilon$	24	38.65	0.4	0.649	116.08
($R^2adj = 25\%$, Var(ε) = 1.52)					
V = Oct-Dec Upwelling prior season					
$ln(S_t) = \alpha + s(ln(N_{t-1})) + \varepsilon$	29.6	44.66			111.57
($R^2adj = 27\%$, Var(ε) = 1.49)					
$ln(S_t) = \alpha + s(ln(N_{t-1})) + \beta V_{t-1} + \varepsilon$	28.6	44.25	0.27	0.604	113.24
($R^2adj = 25\%$, Var(ε) = 1.52)					
$ln(S_t) = \alpha + s(ln(N_{t-1})) + s(V_{t-1}) + \varepsilon$	27.2	43.85	0.18	0.756	114.8
($R^2adj = 23\%$, Var(ε) = 1.56)					
V = Jan-Mar Upwelling prior season					
$ln(S_t) = \alpha + s(ln(N_{t-1})) + \varepsilon$	29.6	44.66			111.57
($R^2adj = 27\%$, Var(ε) = 1.49)					
$ln(S_t) = \alpha + s(ln(N_{t-1})) + \beta V_{t-1} + \varepsilon$	28.6	44.08	0.38	0.54	113.13
($R^2adj = 25\%$, Var(ε) = 1.52)					
$ln(S_t) = \alpha + s(ln(N_{t-1})) + s(V_{t-1}) + \varepsilon$	26.9	42.45	0.62	0.525	114.3
($R^2adj = 25\%$, Var(ε) = 1.53)					

Table B5. Model selection tests of GPCP precipitation as an explanatory variable for the catch during the non-spawning months (Oct-Jun) using 1983 to 2014 data. The data range is determined by the years for which SST was available in order to use a consistent dataset across covariate tests. N_t is the catch during Oct-Jun of season t. V_t is the covariate in the current season which spans two calendar years from July to June in the next year. V_{t-1} is the covariate in the prior Jul-Jun season.

Model	Residual df	Residual deviance	F	p value	AIC
V = Jun-Jul Precipitation					
$ln(N_t) = \alpha + s(ln(N_{t-1})) + s(ln(S_{t-2})) + \varepsilon$	25.6	15.58			80.66
($R^2adj = 61\%$, Var(ε) = 0.59)					
$ln(N_t) = \alpha + s(ln(N_{t-1})) + s(ln(S_{t-2})) + \beta V_t + \varepsilon$	24.6	14.11	2.69	0.115	79.44
($R^2adj = 63\%$, Var(ε) = 0.55)					
$ln(N_t) = \alpha + s(ln(N_{t-1})) + s(ln(S_{t-2})) + s(V_t) + \varepsilon$	22.9	13.77	0.36	0.66	80.94
($R^2adj = 62\%$, Var(ε) = 0.56)					
$ln(N_t) = \alpha + s(ln(N_{t-1})) + s(ln(S_{t-2})) + \beta V_{t-1} + \varepsilon$	24.6	15.54	0.07	0.783	82.49
($R^2adj = 59\%$, Var(ε) = 0.61)					
$ln(N_t) = \alpha + s(ln(N_{t-1})) + s(ln(S_{t-2})) + s(V_{t-1}) + \varepsilon$	22.7	14.09	1.31	0.288	82.1
($R^2adj = 61\%$, Var(ε) = 0.58)					
V = Apr-May Precipitation					
$ln(N_t) = \alpha + s(ln(N_{t-1})) + s(ln(S_{t-2})) + \varepsilon$	25.6	15.58			80.66
($R^2adj = 61\%$, Var(ε) = 0.59)					
$ln(N_t) = \alpha + s(ln(N_{t-1})) + s(ln(S_{t-2})) + \beta V_t + \varepsilon$	24.6	15.42	0.27	0.601	82.28
($R^2adj = 60\%$, Var(ε) = 0.6)					
$ln(N_t) = \alpha + s(ln(N_{t-1})) + s(ln(S_{t-2})) + s(V_t) + \varepsilon$	22.9	14.99	0.41	0.641	83.74
($R^2adj = 59\%$, Var(ε) = 0.61)					
$ln(N_t) = \alpha + s(ln(N_{t-1})) + s(ln(S_{t-2})) + \beta V_{t-1} + \varepsilon$	24.6	15.55	0.05	0.83	82.58
($R^2adj = 59\%$, Var(ε) = 0.61)					
$ln(N_t) = \alpha + s(ln(N_{t-1})) + s(ln(S_{t-2})) + s(V_{t-1}) + \varepsilon$	22.9	15.04	0.5	0.58	83.78
($R^2adj = 59\%$, Var(ε) = 0.62)					

Table B6. Model selection tests of sea surface temperature off Cochi as the explanatory variable (V) for the catch during the non-spawning months (Oct-Jun) using 1983 to 2014 data. See Table B5 for an explanation of the models.

Model	Residual df	Residual deviance	F	p value	AIC
V = Jan-Dec SST					
$ln(N_t) = \alpha + s(ln(N_{t-1})) + s(ln(S_{t-2})) + \varepsilon$ ($R^2 adj = 61\%$, Var(ε) = 0.59)	25.6	15.58			80.66
$ln(N_t) = \alpha + s(ln(N_{t-1})) + s(ln(S_{t-2})) + \beta V_t + \varepsilon$ ($R^2 adj = 68\%$, Var(ε) = 0.48)	24.6	12.34	6.8	0.016	75.14
$ln(N_t) = \alpha + s(ln(N_{t-1})) + s(ln(S_{t-2})) + s(V_t) + \varepsilon$ ($R^2 adj = 67\%$, Var(ε) = 0.49)	22.8	11.96	0.44	0.626	76.63
$ln(N_t) = \alpha + s(ln(N_{t-1})) + s(ln(S_{t-2})) + \beta V_{t-1} + \varepsilon$ ($R^2 adj = 61\%$, Var(ε) = 0.58)	24.6	14.91	1.31	0.263	81.2
$ln(N_t) = \alpha + s(ln(N_{t-1})) + s(ln(S_{t-2})) + s(V_{t-1}) + \varepsilon$ ($R^2 adj = 64\%$, Var(ε) = 0.53)	22.8	12.92	2.12	0.147	79.13
V = Jul-Sep SST					
$ln(N_t) = \alpha + s(ln(N_{t-1})) + s(ln(S_{t-2})) + \varepsilon$ ($R^2 adj = 61\%$, Var(ε) = 0.59)	25.6	15.58			80.66
$ln(N_t) = \alpha + s(ln(N_{t-1})) + s(ln(S_{t-2})) + \beta V_t + \varepsilon$ ($R^2 adj = 66\%$, Var(ε) = 0.5)	24.6	12.89	7.19	0.015	76.47
$ln(N_t) = \alpha + s(ln(N_{t-1})) + s(ln(S_{t-2})) + s(V_t) + \varepsilon$ ($R^2 adj = 73\%$, Var(ε) = 0.4)	23.1	9.78	5.15	0.021	69.77
$ln(N_t) = \alpha + s(ln(N_{t-1})) + s(ln(S_{t-2})) + \beta V_{t-1} + \varepsilon$ ($R^2 adj = 59\%$, Var(ε) = 0.61)	24.6	15.54	0.07	0.78	82.47
$ln(N_t) = \alpha + s(ln(N_{t-1})) + s(ln(S_{t-2})) + s(V_{t-1}) + \varepsilon$ ($R^2 adj = 60\%$, Var(ε) = 0.59)	23.3	14.67	1.07	0.334	82.5

Table B7. Model selection tests of upwelling intensity off Cochi as the explanatory variable. See Table B5 for an explanation of the models.

Model	Residual df	Residual deviance	F	p value	AIC
V = Jul-Sep Upwelling					
$ln(N_t) = \alpha + s(ln(N_{t-1})) + s(ln(S_{t-2})) + \varepsilon$ ($R^2adj = 61\%$, Var(ε) = 0.59)	25.6	15.58			80.66
$ln(N_t) = \alpha + s(ln(N_{t-1})) + s(ln(S_{t-2})) + \beta V_t + \varepsilon$ ($R^2adj = 65\%$, Var(ε) = 0.53)	24.6	13.47	4.15	0.054	77.96
$ln(N_t) = \alpha + s(ln(N_{t-1})) + s(ln(S_{t-2})) + s(V_t) + \varepsilon$ ($R^2adj = 65\%$, Var(ε) = 0.52)	22.8	12.75	0.78	0.453	78.75
$ln(N_t) = \alpha + s(ln(N_{t-1})) + s(ln(S_{t-2})) + \beta V_{t-1} + \varepsilon$ ($R^2adj = 61\%$, Var(ε) = 0.58)	24.6	14.86	1.23	0.276	81.09
$ln(N_t) = \alpha + s(ln(N_{t-1})) + s(ln(S_{t-2})) + s(V_{t-1}) + \varepsilon$ ($R^2adj = 59\%$, Var(ε) = 0.61)	22.8	14.71	0.14	0.844	83.4
V = Oct-Dec Upwelling					
$ln(N_t) = \alpha + s(ln(N_{t-1})) + s(ln(S_{t-2})) + \varepsilon$ ($R^2adj = 61\%$, Var(ε) = 0.59)	25.6	15.58			80.66
$ln(N_t) = \alpha + s(ln(N_{t-1})) + s(ln(S_{t-2})) + \beta V_t + \varepsilon$ ($R^2adj = 60\%$, Var(ε) = 0.6)	24.6	15.36	0.37	0.538	82.15
$ln(N_t) = \alpha + s(ln(N_{t-1})) + s(ln(S_{t-2})) + s(V_t) + \varepsilon$ ($R^2adj = 59\%$, Var(ε) = 0.61)	23.2	14.95	0.5	0.54	83.1
$ln(N_t) = \alpha + s(ln(N_{t-1})) + s(ln(S_{t-2})) + \beta V_{t-1} + \varepsilon$ ($R^2adj = 61\%$, Var(ε) = 0.59)	24.6	15.03	0.94	0.339	81.47
$ln(N_t) = \alpha + s(ln(N_{t-1})) + s(ln(S_{t-2})) + s(V_{t-1}) + \varepsilon$ ($R^2adj = 59\%$, Var(ε) = 0.6)	23.3	14.94	0.12	0.794	82.97
V = Jan-Mar Upwelling					
$ln(N_t) = \alpha + s(ln(N_{t-1})) + s(ln(S_{t-2})) + \varepsilon$ ($R^2adj = 61\%$, Var(ε) = 0.59)	25.6	15.58			80.66
$ln(N_t) = \alpha + s(ln(N_{t-1})) + s(ln(S_{t-2})) + \beta V_t + \varepsilon$ ($R^2adj = 60\%$, Var(ε) = 0.6)	24.6	15.42	0.28	0.588	82.24
$ln(N_t) = \alpha + s(ln(N_{t-1})) + s(ln(S_{t-2})) + s(V_t) + \varepsilon$	23	14.59	0.87	0.412	82.72

Model	Residual df	Residual deviance	F	p value	AIC
($R^2adj = 60\%$, Var(ε) = 0.6)					
$ln(N_t) = \alpha + s(ln(N_{t-1})) + s(ln(S_{t-2})) + \beta V_{t-1} + \varepsilon$	24.6	15.57	0.02	0.887	82.61
($R^2adj = 59\%$, Var(ε) = 0.61)					
$ln(N_t) = \alpha + s(ln(N_{t-1})) + s(ln(S_{t-2})) + s(V_{t-1}) + \varepsilon$	22.9	15.3	0.27	0.725	84.35
($R^2adj = 58\%$, Var(ε) = 0.63)					

Appendix C: Tests for Chlorophyll-a as a covariate

Table C2. Model selection tests of Chlorophyll-a as an explanatory variable for the catch during spawning months (Jul-Sep) using 1998 to 2014 data. The data range is determined by the years for which CHL was available. S_t is the catch during Jul-Sep of season t. V_t is the covariate in the current season which spans two calendar years from July to June in the next year. V_{t-1} is the covariate in the prior Jul-Jun season. For Oct-Dec and Jan-Mar only Chlorophyll-a in the prior season is used since these months are after spawning in the current season. Non-linearity is modeled as a 2nd-order polynomial due to data constraints and appears as $p()$ in the model equations. The non-spawner catch is modeled as a function of non-spawner catch in the prior year only, without spawner catch 2-years prior as in the other covariate analyses (Appendix B). This is done due to data constraints. The models are nested; the roman numeral indicates the level of nestedness. Models at levels II and higher are shown with the component that is added to the base level model (M1) at top.

Model	Residual df	Residual deviance	F	p value	AIC
I-M1: $ln(S_t) = \alpha + p(ln(N_{t-1})) + \varepsilon$	14	1.97			19.6
(R^2adj = 14%, Var(ε) = 0.14)					
V = Jul-Sep Chlorophyll					
II: $ln(S_t) = M1 + \beta V_t$	13	1.68	0.74	0.41	18.93
(R^2adj = 26%, Var(ε) = 0.13)					
III: $ln(S_t) = M1 + p(V_t)$	12	1.68	0.02	0.878	20.89
(R^2adj = 20%, Var(ε) = 0.14)					
IV: $ln(S_t) = M1 + p(V_t) + \beta V_{t-1}$	11	1.67	0.08	0.781	22.76
(R^2adj = 13%, Var(ε) = 0.15)					
V: $ln(S_t) = M1 + p(V_t) + p(V_{t-1})$	10	1.64	0.16	0.694	24.48
(R^2adj = 6%, Var(ε) = 0.16)					
V = Oct-Dec Chlorophyll					
II: $ln(S_t) = M1 + \beta V_{t-1}$	13	1.79	0.12	0.733	19.95
(R^2adj = 21%, Var(ε) = 0.14)					
III: $ln(S_t) = M1 + p(V_{t-1})$	12	1.68	0.73	0.408	20.94
(R^2adj = 20%, Var(ε) = 0.14)					
V = Jan-Mar Chlorophyll					
II: $ln(S_t) = M1 + \beta V_{t-1}$	13	1.79	0.07	0.798	20.02

Model	Residual df	Residual deviance	F	p value	AIC
($R^2 adj$ = 21%, Var(ε) = 0.14)					
III: $ln(S_t) = M1 + p(V_{t-1})$	12	1.77	0.13	0.721	21.83
($R^2 adj$ = 15%, Var(ε) = 0.15)					

Table C1. Model selection tests of Chlorophyll-a as an explanatory variable for the catch during the non-spawning months (Oct-Jun) using 1998 to 2014 data. The data range is determined by the years for which CHL was available. N_t is the catch during Oct-Jun of season t. V_t is the covariate in the current season which spans two calendar years from July to June in the next year. V_{t-1} is the covariate in the prior Jul-Jun season. Non-linearity is modeled as a 2nd-order polynomial due to data constraints and appears as $p()$ in the model equations. The non-spawner catch is modeled as a function of non-spawner catch in the prior year only, without spawner catch 2-years prior as in the other covariate analyses (Appendix B). This is done due to data constraints. The models are nested; the roman numeral indicates the level of nestedness. Models at levels II and higher are shown with the component that is added to the base level model (M1) at top.

Model	Residual df	Residual deviance	F	p value	AIC
I-M1: $ln(N_t) = \alpha + p(ln(N_{t-1})) + \varepsilon$	14	1.97			19.6
($R^2 adj$ = 14%, Var(ε) = 0.14)					
V = Jul-Sep Chlorophyll					
II: $ln(N_t) = M1 + \beta V_t$	13	1.96	0.06	0.815	21.52
($R^2 adj$ = 8%, Var(ε) = 0.15)					
III: $ln(N_t) = M1 + p(V_t)$	12	1.87	0.54	0.478	22.69
($R^2 adj$ = 5%, Var(ε) = 0.16)					
II: $ln(N_t) = M1 + \beta V_{t-1}$	13	1.92	0.32	0.582	21.17
($R^2 adj$ = 10%, Var(ε) = 0.15)					
III: $ln(N_t) = M1 + p(V_{t-1})$	11.6	1.87	0.22	0.731	22.75
($R^2 adj$ = 4%, Var(ε) = 0.16)					
V = Oct-Dec Chlorophyll					
II: $ln(N_t) = M1 + \beta V_t$	13	1.88	0.77	0.402	20.84
($R^2 adj$ = 11%, Var(ε) = 0.14)					
III: $ln(N_t) = M1 + p(V_t)$	12	1.71	1.55	0.241	21.17
($R^2 adj$ = 13%, Var(ε) = 0.14)					
IV: $ln(N_t) = M1 + p(V_t) + \beta V_{t-1}$	11	1.14	4.99	0.05	16.37
($R^2 adj$ = 36%, Var(ε) = 0.1)					
V: $ln(N_t) = M1 + p(V_t) + p(V_{t-1})$	10	1.13	0.12	0.733	18.16
($R^2 adj$ = 31%, Var(ε) = 0.11)					
II: $ln(N_t) = M1 + \beta V_{t-1}$	13	1.5	4.32	0.063	16.96

Model	Residual df	Residual deviance	F	p value	AIC
($R^2 adj$ = 29%, Var(ε) = 0.12)					
III: $ln(N_t) = M1 + p(V_{t-1})$	10.3	1.2	1.03	0.409	17.14
($R^2 adj$ = 33%, Var(ε) = 0.11)					
V = Jan-Mar Chlorophyll					
II: $ln(N_t) = M1 + \beta V_t$	13	1.97	0	0.972	21.6
($R^2 adj$ = 7%, Var(ε) = 0.15)					
III: $ln(N_t) = M1 + p(V_t)$	12	1.82	0.93	0.358	22.23
($R^2 adj$ = 7%, Var(ε) = 0.15)					
II: $ln(N_t) = M1 + \beta V_{t-1}$	13	1.67	2.14	0.171	18.78
($R^2 adj$ = 21%, Var(ε) = 0.13)					
III: $ln(N_t) = M1 + p(V_{t-1})$	11	1.63	0.12	0.884	21.25
($R^2 adj$ = 14%, Var(ε) = 0.14)					

Table C3. Model selection tests of Chlorophyll-a as an explanatory variable for the catch during the non-spawning months (Oct-Jun) using box 5.

Model	Residual df	Residual deviance	F	p value	AIC
I-M1: $ln(N_t) = \alpha + p(ln(N_{t-1})) + \varepsilon$	14	1.97			19.6
($R^2 adj$ = 14%, Var(ε) = 0.14)					
V = Jul-Sep Chlorophyll					
II: $ln(N_t) = M1 + \beta V_t$	13	1.67	2.01	0.187	18.76
($R^2 adj$ = 21%, Var(ε) = 0.13)					
III: $ln(N_t) = M1 + p(V_t)$	12	1.66	0.05	0.836	20.69
($R^2 adj$ = 15%, Var(ε) = 0.14)					
II: $ln(N_t) = M1 + \beta V_{t-1}$	13	1.91	0.46	0.512	21.04
($R^2 adj$ = 10%, Var(ε) = 0.15)					
III: $ln(N_t) = M1 + p(V_{t-1})$	10.5	1.53	1.09	0.383	21.19
($R^2 adj$ = 15%, Var(ε) = 0.14)					
V = Oct-Dec Chlorophyll					
II: $ln(N_t) = M1 + \beta V_t$	13	1.55	4.22	0.067	17.57
($R^2 adj$ = 27%, Var(ε) = 0.12)					
III: $ln(N_t) = M1 + p(V_t)$	12	1.35	2.11	0.177	17.13
($R^2 adj$ = 31%, Var(ε) = 0.11)					
IV: $ln(N_t) = M1 + p(V_t) + \beta V_{t-1}$	11	1	3.51	0.091	14.1
($R^2 adj$ = 44%, Var(ε) = 0.09)					
V: $ln(N_t) = M1 + p(V_t) + p(V_{t-1})$	10	0.98	0.18	0.684	15.8
($R^2 adj$ = 40%, Var(ε) = 0.1)					
II: $ln(N_t) = M1 + \beta V_{t-1}$	13	1.37	5.15	0.044	15.47
($R^2 adj$ = 35%, Var(ε) = 0.11)					
III: $ln(N_t) = M1 + p(V_{t-1})$	11	1.35	0.11	0.895	17.89
($R^2 adj$ = 29%, Var(ε) = 0.12)					
V = Jan-Mar Chlorophyll					
II: $ln(N_t) = M1 + \beta V_t$	13	1.59	3.35	0.097	17.92
($R^2 adj$ = 25%, Var(ε) = 0.12)					

Model	Residual df	Residual deviance	F	p value	AIC
III: $ln(N_t) = M1 + p(V_t)$	12	1.57	0.17	0.692	19.72
(R^2adj = 20%, Var(ε) = 0.13)					
II: $ln(N_t) = M1 + \beta V_{t-1}$	13	1.72	2.78	0.125	19.33
(R^2adj = 19%, Var(ε) = 0.13)					
III: $ln(N_t) = M1 + p(V_{t-1})$	10.4	0.98	3.25	0.071	13.58
(R^2adj = 46%, Var(ε) = 0.09)					

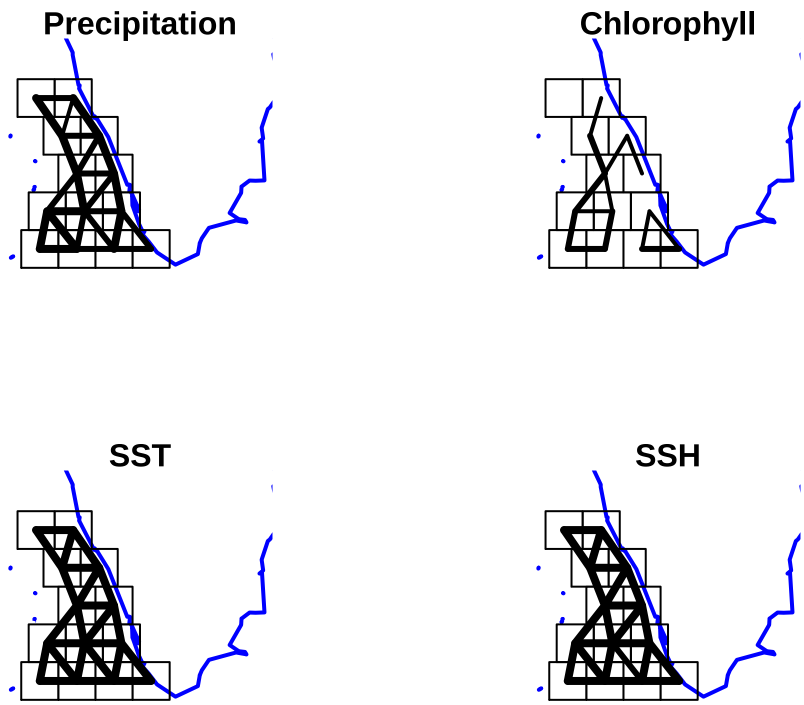

Figure C1. Correlation of the covariates across boxes. Correlation is shown by the width of the lines between neighboring boxes.

Appendix D: Correlation of covariates across the boxes

Appendix E: Covariates along the SE India coast

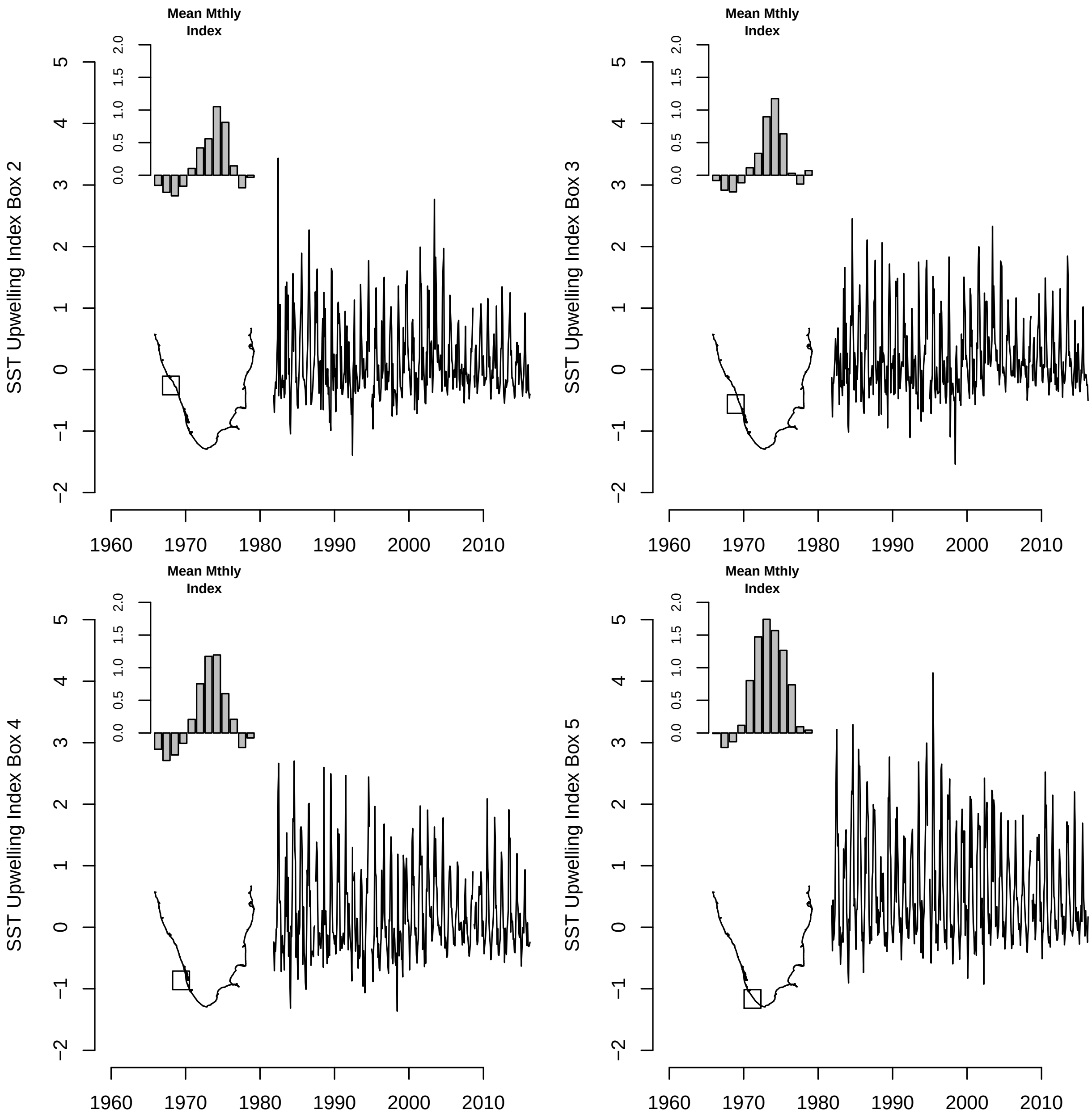

Figure E1. Upwelling index.

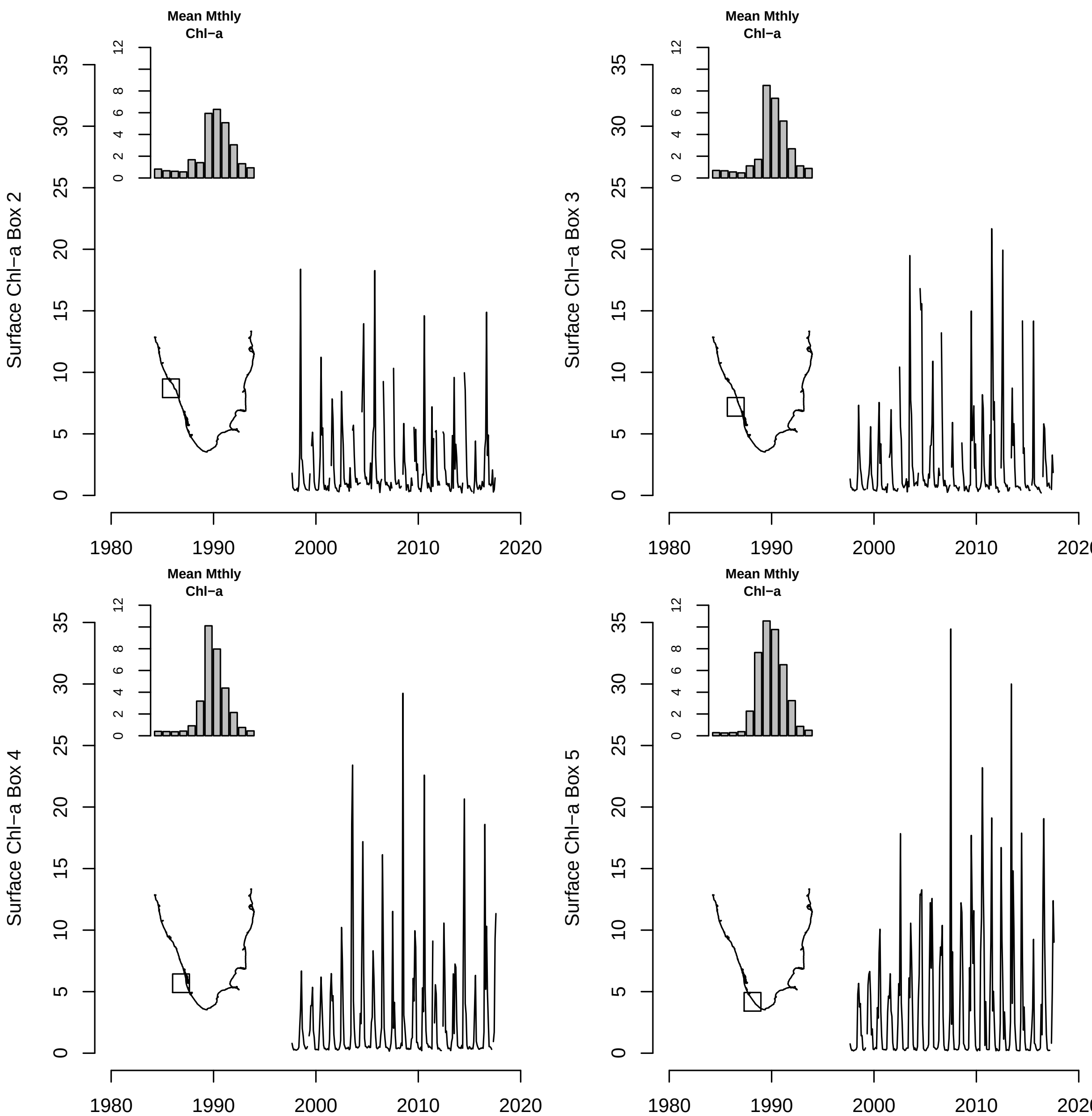

Figure E2. Chlorophyll-a.

Appendix F: Comparison of land and oceanic rainfall measurements

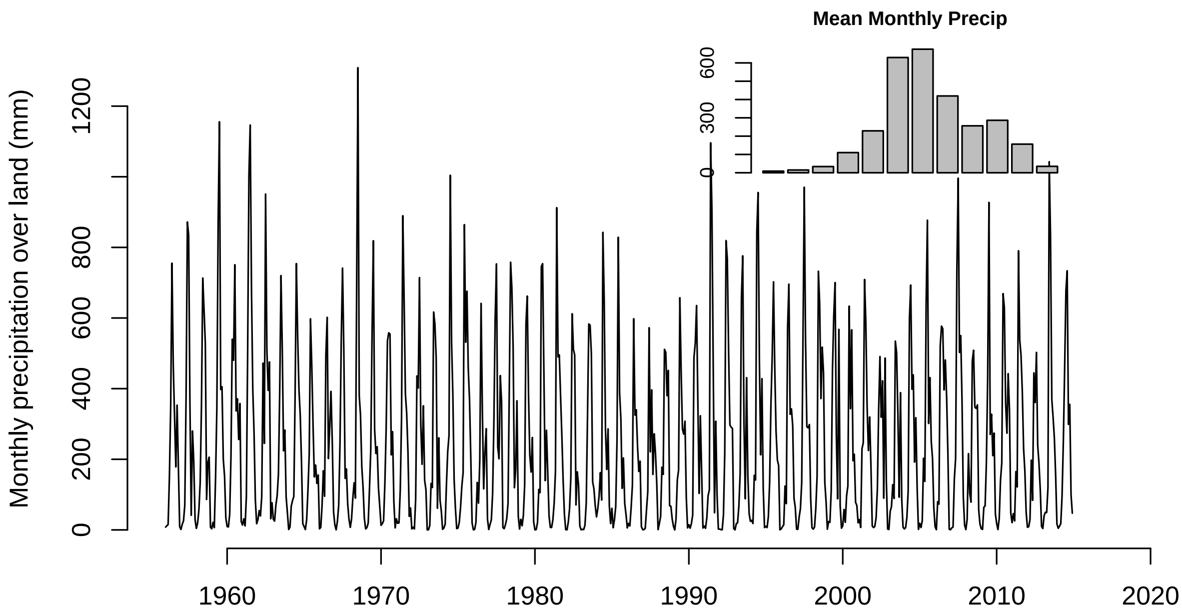
Mean Monthly Precip
0
300
600
Monthly precipitation over land (mm)
0
200
400
600
800
1200
1960
1970
1980
1990
2000
2010
2020

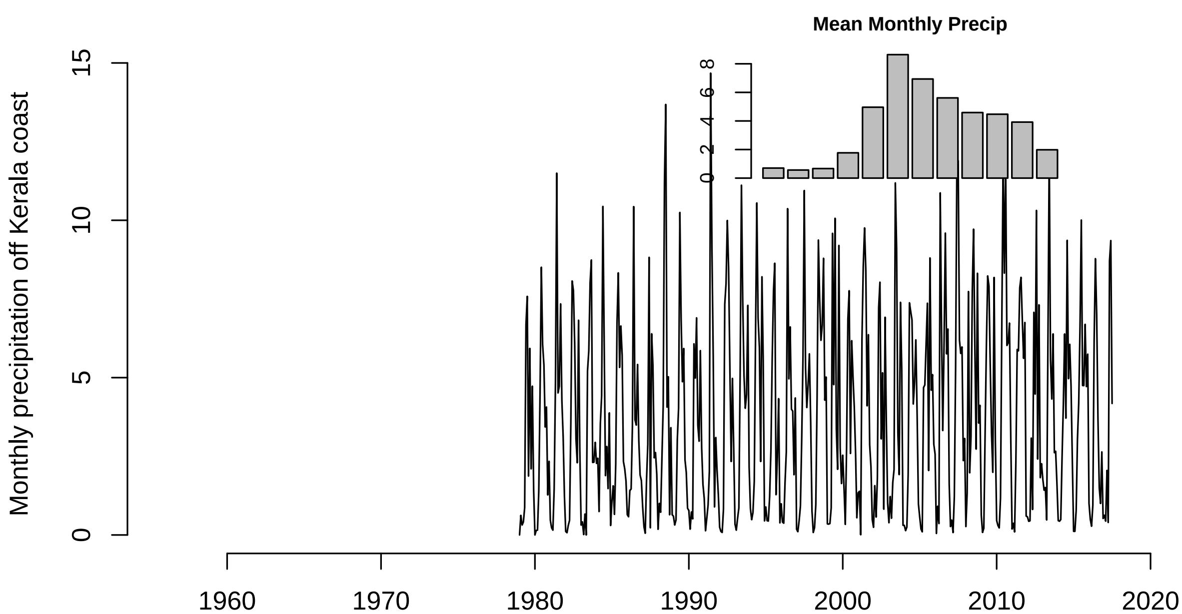
Mean Monthly Precip
0
2
4
6
8
Monthly precipitation off Kerala coast
0
5
10
15
1960
1970
1980
1990
2000
2010
2020

Figure F1

Appendix G: Chlorophyll-a images in 2016

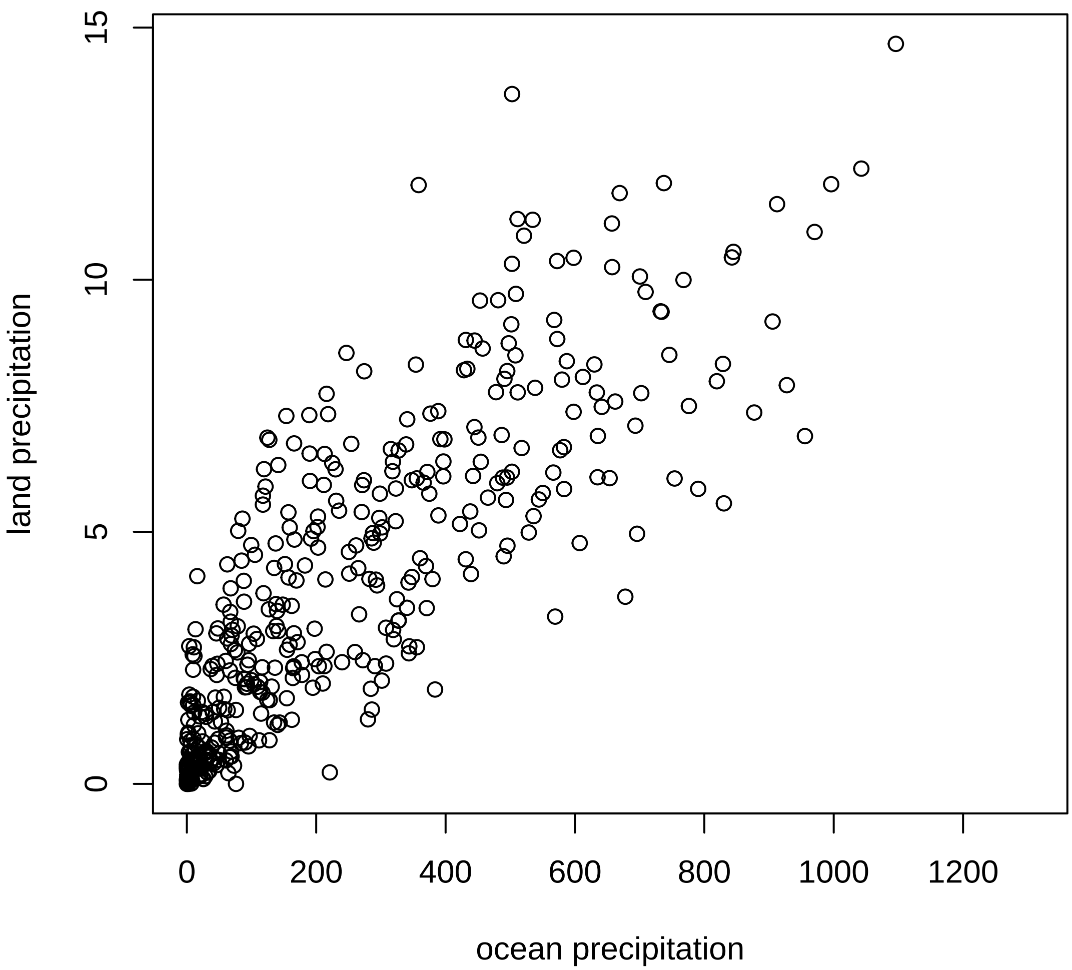

Figure F2. Monthly precipitation measured over land via land gauges versus the precipitation measured via remote sensing over the ocean.

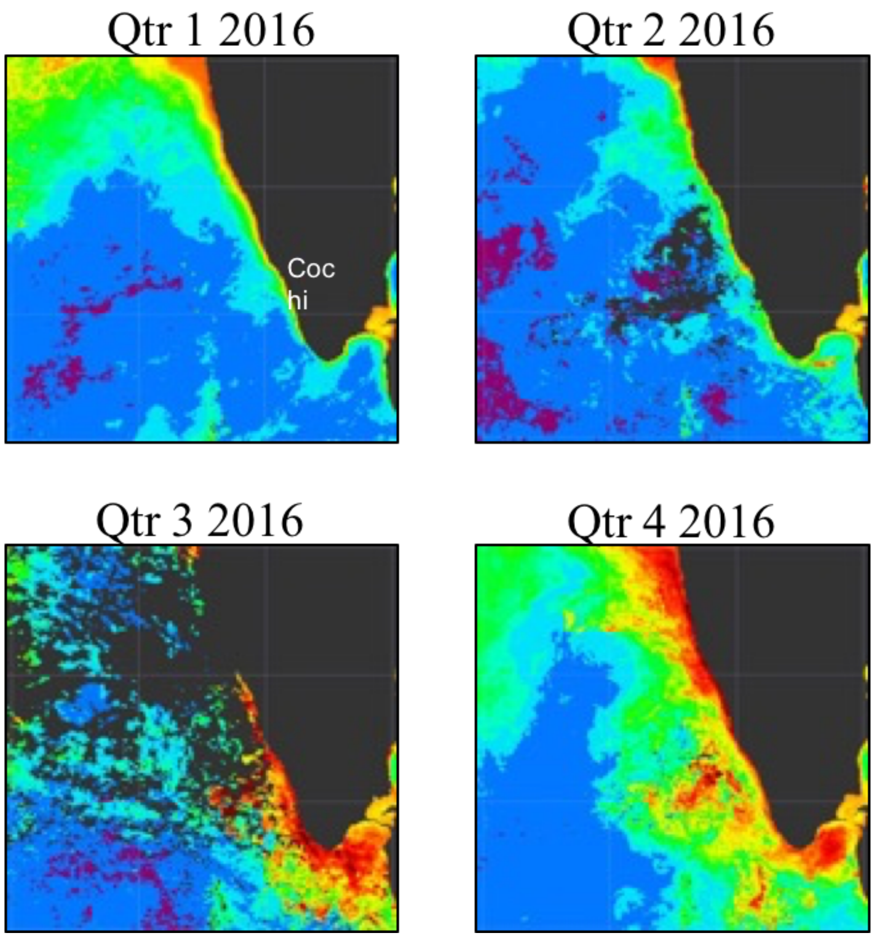

Figure 9